https://doi.org/10.5194/egusphere-2025-6076
Preprint. Discussion started: 4 February 2026


# Sensitivity and Uncertainty Analysis of China's Terrestrial Carbon-Water Cycle Using a Dynamic Global Vegetation Model

**Fulai Feng [a], Jianwu Yan [a*], Wei Liang [a], Xiaohong Liu [a], Bo Liu [a], Xiaoru Liang [a], Jia Wei [a], Yangcan Bao [a]**

[a] School of Geography and Tourism, Shaanxi Normal University, Xi'an, 710119, China

Corresponding author: Jianwu Yan (yanjw@snnu.edu.cn)

https://doi.org/10.5194/egusphere-2025-6076
Preprint. Discussion started: 4 February 2026



# Abstract

Parameter uncertainty in Dynamic Global Vegetation Models (DGVMs) substantially impacts the reliability of carbon-water cycle simulations. Using the LPJ-GUESS model at 13 sites across China's diverse ecosystems, this study employed a multi-method (Morris, eFAST, Sobol') sensitivity analysis on 39 key parameters to assess their impacts on nine carbon-water cycle variables. Our results revealed that the model's behavior is co-dominated by both core physiological parameters, often hard-coded in the source, and plant functional type-specific traits. This finding suggests limitations in the common practice of focusing calibration solely on user-adjusted files. Furthermore, these parameter controls are highly context-dependent, shifting based on both the target process (e.g., carbon uptake as opposed to water flux) and the regional climate, where arid ecosystems respond most strongly to water-use parameters. The multi-method approach also highlighted that the influence of many parameters is mediated through complex interactions rather than direct effects alone. Consequently, this complex web of sensitivities propagates into contrasting patterns of model uncertainty: arid ecosystems exhibit the highest relative uncertainty, making predictions more uncertain, while humid, productive ecosystems show the largest absolute uncertainty, posing a challenge for carbon budgeting. These findings provide a scientific basis for developing targeted, region-specific parameterization strategies to reduce model uncertainty and improve assessments of terrestrial carbon sink functions.


**Keywords**

Sensitivity analysis; Uncertainty analysis; Carbon-water cycle; Parameterization; LPJ-GUESS

https://doi.org/10.5194/egusphere-2025-6076
Preprint. Discussion started: 4 February 2026


# 1 Introduction

Terrestrial ecosystems are an important component of the global carbon cycle and water cycle, and play a crucial role in regulating climate change through land–atmosphere interactions (Buster et al., 2024). Carbon uptake and water transport are tightly coupled through plant physiological processes, especially via stomatal regulation, which simultaneously controls carbon dioxide assimilation and water transpiration. In turn water availability directly restricts photosynthetic efficiency, affecting carbon assimilation, vegetation structure, and then feedbacks to soil moisture and evapotranspiration (Hickler et al., 2015). Together, these processes form a complex and dynamic carbon-water coupling system linking terrestrial ecosystems and the atmosphere (Buster et al., 2024; Zhao et al., 2025).

Dynamic Global Vegetation Models (DGVMs) are process-based tools that are widely used to simulate ecosystem structure and function under varying climate conditions (Bonan et al., 2003; Forster et al., 2024; Liu et al., 2024). Among them, the Lund-Potsdam-Jena General Ecosystem Simulator (LPJ-GUESS) has become an important platform for carbon-water dynamic modeling research due to its explicit representation of plant functional types, biogeochemical cycles and hydrological processes (Smith et al., 2001). The model can simulate key ecological variables such as gross primary productivity (GPP), evapotranspiration (ET), vegetation carbon storage, and soil carbon storage, and has been widely used at both global and regional scales (Smith et al., 2014; Smith et al., 2011).

Despite their broad applicability, the performance of DGVMs is strongly dependent on parameter settings to describe ecological processes, and the selection of parameter values is subject to uncertainty (Verrelst et al., 2019), especially in areas characterized by pronounced ecological heterogeneity. China encompasses a wide range of climate zones and vegetation types (Chen et al., 2022), spanning humid monsoon regions in the southeast to arid and semi-arid inland regions in the northwest. This spatial heterogeneity poses a challenge to the adaptability of model parameters (Guan et al., 2023; Wu, 2023; Ma et al., 2022b), and also provides an ideal platform for exploring regional differences in parameter sensitivity of carbon-water coupling processes.

Model parameter sensitivity analysis is a critical method to identify key parameters driving model output and improve simulation accuracy and credibility (Yuxi et al., 2024). At present,

https://doi.org/10.5194/egusphere-2025-6076
Preprint. Discussion started: 4 February 2026


sensitivity analysis methods have evolved from traditional one-at-a-time (OTA) variation to global sensitivity analysis techniques, such as Morris, eFAST and Sobol', which can identify nonlinear relationships and parameter interaction effects (Ma et al., 2022b; Nossent et al., 2011; Vazquez-Cruz et al., 2014). Although these methods have been increasingly applied in ecosystem modeling studies (Pappas et al., 2013), most of them have focused on individual carbon cycle processes or site-specific analyses, with relatively limited attention to the integrated evaluation of carbon-water coupling processes (Oberpriller et al., 2022).

Previous studies have shown that LPJ-GUESS outputs are highly sensitive to parameters such as photosynthetic efficiency, plant structure, and carbon allocation strategies. For instance, Pappas et al. (2013) highlighted the influence of photosynthetic quantum efficiency and canopy scale conversion coefficient on GPP and NPP, while Oberpriller et al. (2022) emphasized that the parameters related to water processes and climatic drivers, such as temperature and precipitation, substantially affects on forest simulations. However, these studies are largely confined to temperate regions in Europe, and offer limited insights into the spatial variability of parameter sensitivities across China's ecologically heterogeneous landscapes. Moreover, calibration and sensitivity analyses in the DGVM community have traditionally focused on the more accessible Plant Functional Type (PFT) parameters found in user-facing files, whereas the influence of core physiological parameters embedded within the model's source code remains less well quantified, potentially limiting a comprehensive understanding of model behavior (Peng et al., 2024). Furthermore, different sensitivity analysis methods have their strengths and limitations. The Morris method has high computational efficiency but is difficult to evaluate interaction effects, whereas the Sobol' method can quantify both main effects and interaction effects but has high computational costs. The extent to which these methods converge or diverge is not well understood, particularly in their ability to untangle direct, linear parameter effects from the complex, non-linear interactions that likely govern coupled systems. More importantly, most existing studies focus on carbon cycle variables, often neglecting the critical role of water dynamics and their feedbacks within ecosystem simulations (Oberpriller et al., 2022).

To address these gaps, this study selected 13 representative ecosystem sites across China, covering a variety of typical vegetation types and climate zones. Based on the LPJ-GUESS model, three complementary sensitivity analysis methods--Morris, eFAST and Sobol'--were used to systematically evaluate the impact of 39 key ecological process parameters on the carbon and

https://doi.org/10.5194/egusphere-2025-6076
Preprint. Discussion started: 4 February 2026


water cycle simulation results. By assessing the sensitivity of nine carbon and water cycle variables and analyzing the spatial heterogeneity of parameter effects, this study aims to (1) identify the dominant parameters driving model outputs, (2) evaluate the regional variability of parameter sensitivities, (3) compare the consistency and complementarity of sensitivity analysis methods, and (4) quantify uncertainty propagation across ecosystems. The findings are intended to support the refinement of parameterization strategies in DGVMs and enhance the model's regional carbon–water cycle assessments under future climate scenarios.

# 2 Materials and Methods

## 2.1 Study Area and Site Design

To assess the parameter sensitivity of the LPJ-GUESS model across diverse ecosystems, this study selected 13 representative sites spanning the major natural vegetation types and climate zones in China (Fig. 1; see Table S1 in the Supporting Information for site details). These sites, located within national nature reserves, were selected to minimize anthropogenic disturbances and ensure ecological representativeness.

Site selection was primarily based on the MODIS MCD12Q1 land cover product (2001-2023) (Friedl & Sulla-Menashe, 2022) and boundary data of Chinese nature reserves. Key criteria for the site selection included: ensuring the sites represent dominant regional vegetation types (e.g., forests, grasslands); excluding areas of significant anthropogenic land use; and verifying vegetation stability over time by assessing land cover consistency from 2001 to 2023.

To enhance national-scale representativeness, a two-stage sampling strategy was adopted, combining the International Geosphere–Biosphere Programme (IGBP) vegetation type classification with a spatial equilibrium algorithm to ensure a balanced geographical distribution. A detailed description of the site selection process is provided in Text S1 in the Supporting Information.

https://doi.org/10.5194/egusphere-2025-6076
Preprint. Discussion started: 4 February 2026


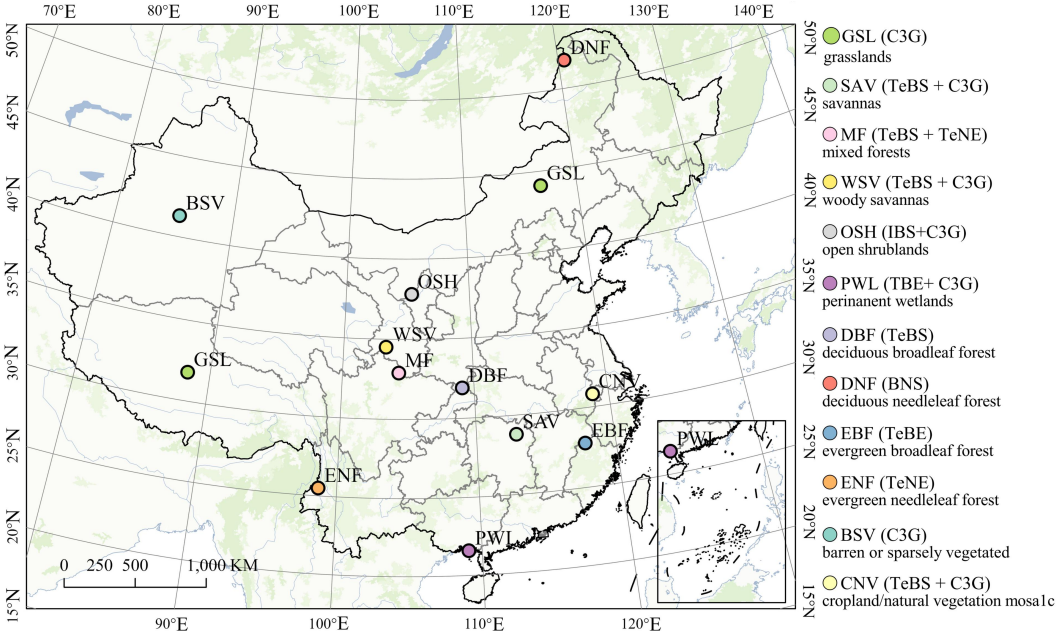


**Fig. 1. Spatial distribution of sample points used for sensitivity analysis**

## 2.2 Model and Driving Data

### 2.2.1 LPJ-GUESS Model

LPJ-GUESS is a process-based Dynamic Global Vegetation Model designed to simulate terrestrial ecosystem dynamics under changing environmental conditions (Sitch et al., 2003; Smith et al., 2014). It explicitly represents key water, carbon, and nitrogen processes within the soil-plant-atmosphere continuum and simulates vegetation competition for light, water, and space resources (Lindeskog et al., 2013; Lindeskog et al., 2021). The model classifies vegetation into 12 PFTs characterized by specific growth forms (e.g., herbaceous, broadleaf tree, deciduous tree), photosynthetic pathways (C3 or C4), phenological strategies (evergreen, summergreen, or raingreen), tree biometrics and life-history traits, as well as bioclimatic constraints on establishment and survival (Olin et al., 2015; Smith et al., 2014). It also accounts for the fire sensitivity and disturbance responses among PFTs (Smith et al., 2014).

In this study, LPJ-GUESS version 4.1 was employed in cohort mode, in which woody individuals of the same size and age within a local neighborhood or patch are grouped into a representative average individual. Each PFT is simulated as a set of such cohorts, assuming

https://doi.org/10.5194/egusphere-2025-6076
Preprint. Discussion started: 4 February 2026


structural uniformity among individuals of the same age within a patch (Olin et al., 2015; Pugh et al., 2019; Teckentrup, 2023). Establishment, mortality, and disturbance events are governed by stochastic processes. Fire occurrence is simulated annually (stochastically) based on probabilistic functions of temperature, fuel availability, and upper soil moisture content, which served as a proxy for litter moisture (Thonicke et al., 2001).

### 2.2.2 Driving Data

The driving data required by the LPJ-GUESS model include monthly meteorological variables (temperature, precipitation, and incoming shortwave radiation), soil texture (assumed static over time), annual atmospheric $CO_2$ concentration, and nitrogen deposition rates.

In this study, meteorological forcing data were derived from the ERA5-Land reanalysis dataset, which provides monthly data at a spatial resolution of 0.1° for the period 1980-2023 (Copernicus Climate Change Service, 2019). Specifically, monthly average temperature, cumulative precipitation, and average incident shortwave radiation were extracted. Annual atmospheric $CO_2$ concentration data, reflecting interannual variability, were derived from long-term observations at the Mauna Loa Observatory, Hawaii (Lan et al., 2023). Soil texture data, including sand and clay content, carbon-nitrogen ratio, pH, soil bulk density, and soil organic carbon, were obtained from the National Tibetan Plateau Data Center (Shi et al., 2025). For consistency, values from six standard soil layers within the 0-2 meters depth range were averaged to generate a single representative soil profile for each site. Nitrogen deposition data were adopted from the Lamarque dataset (default spatial resolution of 0.5°), with values from the nearest grid cell assigned to each site as model input (Lamarque et al., 2013).

### 2.2.3 Model Setup

To ensure the stabilization of ecosystem carbon pools, the LPJ-GUESS model was initialized with a 500-year spin-up period. This period employed repeated cycling of the first 20 years (1980-2000) of climate forcing data, with temperature trends removed to maintain climatic baseline. During the spin-up, stochastic processes such as fire and natural disturbances were enabled to represent inherent ecological dynamics. However, anthropogenic land-use changes were excluded, as all selected sites are located within national nature reserves, where direct human impacts are minimal.

https://doi.org/10.5194/egusphere-2025-6076
Preprint. Discussion started: 4 February 2026


## 2.3 Parameter Selection and Value Ranges

For the sensitivity analysis, 39 key parameters of the LPJ-GUESS model were selected, covering fundamental ecological processes such as photosynthesis, carbon allocation, and vegetation structure. These parameters comprise 19 core physiological parameters, which are applied uniformly across all vegetation types, and 20 PFT specific traits that characterize the strategies of individual ecosystems. Detailed information on parameter definitions, functions, and value ranges, is provided in Table 1.

Parameter value ranges were defined based on a combination of sources: (1) default values and annotations within the model source code; (2) empirical ranges reported in peer-reviewed LPJ-GUESS calibration studies; and (3) a ±25% deviation from the default value where direct empirical constraints were unavailable. This strategy was adopted to ensure that the parameter ranges are both sufficiently broad to support global sensitivity analysis and consistent with current ecological understanding.

It is crucial to distinguish the objective of this study—Global Sensitivity Analysis (GSA)—from that of parameter calibration. For several hard-coded internal parameters (e.g., *reprfrac, turnover_root*), value ranges were defined using their technically permissible bounds [0, 1] as specified in the model source code. We acknowledge that the extreme values within these bounds may not always correspond to ecologically realistic conditions. However, retaining these full technical ranges is appropriate in the context of GSA for two reasons. First, empirical ecological constraints for these internal parameters are currently lacking, and restricting their ranges without supporting evidence would introduce subjective assumptions. Second, GSA is intended to examine model sensitivity across the technically allowable parameter space, rather than to infer parameter realism. In this context, strong sensitivity associated with poorly constrained parameters is interpreted as a diagnostic indicator of model behavior, rather than as a direct measure of real-world uncertainty, and may point to priorities for future model development and structural refinement. Finally, for all sampling procedures, parameter values were drawn independently from uniform distributions within their specified minimum and maximum ranges, reflecting the absence of prior information on parameter probability distributions.

https://doi.org/10.5194/egusphere-2025-6076
Preprint. Discussion started: 4 February 2026


192

Table 1. Parameters for Sensitivity Analysis

| Parameter Name | Default Value | Minimum Value | Maximum Value | Physical Meaning | Literature sources |
|---|---|---|---|---|---|
| THETA | 0.7 | 0.2 | 0.996 | colimitation (shape) parameter | (Collatz et al., 1990; Leverenz, 1988) |
| ALPHAA | 0.5 | 0.3 | 0.7 | scaling factor for PAR absorption from leaf to plant projective area level | (Haxeltine & Prentice, 1996) |
| ALPHA_C3 | 0.08 | 0.02 | 0.125 | intrinsic quantum efficiency of CO2 uptake, C3 plants | (Farquhar et al., 1980; Hallgren & Pitman, 2000) |
| ALPHA_C4 | 0.053 | 0.0477 | 0.0583 | intrinsic quantum efficiency of CO2 uptake, C4 plants | (Ehleringer & Björkman, 1977) |
| BC3 | 0.015 | 0.01 | 0.021 | leaf respiration as fraction of maximum rubisco, C3 plants | (Farquhar et al., 1980; Hallgren & Pitman, 2000) |
| BC4 | 0.02 | 0.018 | 0.022 | leaf respiration as fraction of maximum rubisco, C4 plants | - |
| GM | 3.26 | 2.5 | 18.5 | Maximum canopy conductance equivalent | (Magnani et al., 1998) |
| ALPHAM | 1.391 | 1.1 | 1.5 | Empirical parameter in evapotranspiration process | (Monteith, 1995) |
| TAU_LITTER | 2.85 | 1.23 | 5.26 | Litter decomposition time at 10°C | (Meentemeyer, 1978) |
| ATMFRAC | 0.7 | 0.5 | 0.9 | Fraction of litter decomposition entering fast soil organic matter pool | (Pappas et al., 2013) |
| FASTFRAC | 0.985 | 0.85 | 0.99 | Fraction of bound litter decomposition entering intermediate soil pool | (Zaehle et al., 2005) |
| PRIESTLEY_TAYLOR | 1.32 | 1.08 | 1.6 | Priestley-Taylor coefficient (converts equilibrium ET to potential ET) | (Pappas et al., 2013; Sumner & Jacobs, 2005) |
| BETA | 0.17 | 0.15 | 0.19 | Global average of shortwave albedo (not vegetation-specific) | (Li et al., 2022) |
| FRADPAR | 0.5 | 0.4 | 0.7 | Fraction of net incoming shortwave radiation that is photosynthetically active (PAR) | - |
| MINFUEL | 0.2 | 0.01 | 0.4 | Minimum abovegroundlitter mass required for fire occurrence | (Zaehle et al., 2005) |
| K_MORT1 | 0.01 | 0.005 | 0.1 | Constant in tree mortality equation | (Zaehle et al., 2005) |
| K_MORT2 | 35 | 20 | 50 | Constant in tree mortality equation based on annual NPP and growth efficiency | (Zaehle et al., 2005) |
| R_GROWTH | 0.25 | 0.15 | 0.4 | Growth respiration | (Sprugel et al., 1995) |

| | | | | | |
|---|---|---|---|---|---|
| common_lambda_max | 0.8 | 0.6 | 0.8 | Ratio of intercellular to ambient $CO_2$concentration under no water stress | (Haxeltine & Prentice, 1996) |
| common_emax | 5 | 2.4 | 6.2 | Maximum evapotranspiration rate | (Pappas et al., 2013; Whitehead et al., 1994) |
| common_reprfrac | 0.1 | 0 | 1 | Fraction of NPP allocated to reproduction | SourceCode |
| tree_turnover_root | 0.7 | 0 | 1 | Fine root turnover rate (annual fraction) | SourceCode |
| tree_k_rp | 1.6 | 1.33 | 1.6 | Constant in tree allometric growth equation | (Enquist & Niklas, 2002; Whitehead et al., 1994) |
| tree_crownarea_max | 50 | 30 | 60 | Maximum tree crown area ($m^2$) | - |
| tree_litterme | 0.3 | 0.0225 | 0.375 | Moisture flammability threshold of tree litter (as a fraction of available water capacity) | - |
| tree_k_allom2 | 60 | 5 | 60 | Constant in tree allometric growth equation | - |
| tree_k_allom3 | 0.67 | 0.5 | 0.8 | Constant in tree allometric growth equation | (Zaehle et al., 2005) |
| tree_kest_bg | 0.1 | 0 | 1 | Constant in tree establishment rate equation | SourceCode |
| broadleaved_gmin | 0.5 | 0.42 | 0.58 | Minimum stomatal conductance of broadleaved canopy | (Körner, 1995; Zaehle et al., 2005) |
| needleleaved_gmin | 0.3 | 0.22 | 0.38 | Minimum stomatal conductance of needleleaved canopy | (Körner, 1995; Zaehle et al., 2005) |
| broadleaved_k_allom1 | 250 | 225 | 275 | Constant in broadleaved tree allometric growth equation | - |
| grass_gmin | 0.5 | 0.22 | 0.38 | Minimum stomatal conductance of grass canopy | (Körner, 1995) |
| needleleaved_k_allom1 | 150 | 112.5 | 187.5 | Constant in needleleaved tree allometric growth equation | - |
| shade_tolerant_est_max | 0.05 | 0.05 | 0.48 | Maximum seedling establishment rate for shade-tolerant species | (Pappas et al., 2013; Zaehle et al., 2005) |
| shade_intolerant_est_max | 0.2 | 0.05 | 0.48 | Maximum seedling establishment rate for shade-intolerant species | (Pappas et al., 2013; Zaehle et al., 2005) |
| grass_litterme | 0.2 | 0.15 | 0.25 | Moisture flammability threshold of grass litter (as a fraction of available water capacity) | - |
| broadleaved_k_latosa | 6000 | 2000 | 8000 | Ratio of leaf area to sapwood area in broadleaved trees | (Oberpriller et al., 2022; Zaehle et al., 2005) |
| needleleaved_k_latosa | 5000 | 2000 | 8000 | Ratio of leaf area to sapwood area in needleleaved trees | (Oberpriller et al., 2022; Zaehle et al., 2005) |

Note:sourcecode indicates that the range was derived from the source code



https://doi.org/10.5194/egusphere-2025-6076
Preprint. Discussion started: 4 February 2026

https://doi.org/10.5194/egusphere-2025-6076
Preprint. Discussion started: 4 February 2026


## 2.4 Sensitivity Analysis Methods

This study applies three complementary sensitivity analysis methods to assess the impact of parameters on simulated outputs from different analytical perspectives.

### 2.4.1 Morris Sensitivity Analysis Method

The Morris method is an efficient global sensitivity analysis technique commonly designed for preliminary parameter screening. It is based on a One-Factor-At-a-Time (OAT) perturbation scheme, in which parameters are varied individually along predefined trajectories in the parameter space while other parameters remain fixed for each elementary step (Morris, 1991). By constructing multiple such trajectories, the method estimates the Elementary Effects (*EE*) of parameters through successive single-parameter perturbations:

$$EE_i = \frac{f(x_1, \ldots, x_{i-1}, x_i + \Delta, x_{i+1}, \ldots, x_N) - f(x_1, \ldots, x_i, \ldots, x_N)}{\Delta} \quad (1)$$

where $f(\cdot)$ is the model output, and $x$ and $x+\Delta$ represent the function values at points before and after only the *i-th* parameter is changed, respectively. This definition reflects the impact on the output results when only the *i-th* factor undergoes a minor perturbation.

The Morris method characterizes parameter importance using two summary statistics. The mean of elementary effects ($\mu$) represents the overall influence magnitude of a parameter on model outputs, while the standard deviation of the elementary effects ($\sigma$) captures the variability of this influence across the parameter space, which may arise from non-linear responses and interactions with other parameters.

### 2.4.2 eFAST Sensitivity Analysis Method

The extended Fourier Amplitude Sensitivity Test (eFAST) is a variance-based global sensitivity analysis method used to quantify the relative importance of model input parameters (Saltelli et al., 1999; Andrea Saltelli, 2002). The method explores the parameter space by assigning sinusoidal functions with distinct frequencies to each parameter, which allows the decomposition of output variance into contributions associated with individual parameter:

https://doi.org/10.5194/egusphere-2025-6076
Preprint. Discussion started: 4 February 2026


$$V_Y = \sum_i V_i + \sum_{i<j} V_{ij} + \sum_{i<j<k} V_{ijk} + \cdots + V_{12\ldots k} \quad (2)$$

The eFAST method calculates two key types of sensitivity indices: First-order sensitivity index $S_i$:

The proportion of contribution from the direct effect of the parameter:

$$S_i = \frac{V_i}{V(Y)} \quad (3)$$

Total sensitivity index $ST_i$: The overall contribution including all interaction effects:

$$ST_i = 1 - \frac{V_{-i}}{V(Y)} \quad (4)$$

This approach is well suited for the analysis of non-linear models behavior, as it can capture both first-order (main effect) sensitivities and higher-order (interaction) contributions arising from parameter interactions, while maintaining a relatively moderate computational cost (Saltelli et al., 1999; Vazquez-Cruz et al., 2014).

### 2.4.3 Sobol' Sensitivity Analysis Method

The Sobol' method is a rigorous global sensitivity analysis framework that decomposes the total variance of model outputs into contributions from individual input parameters and their interactions through Monte Carlo sampling (Sobol′, 2001). It provides a detailed quantification of both first-order and higher-order sensitivity effects, making it particularly suitable for complex, nonlinear, and non-monotonic models. In this method, two key sensitivity indices are calculated (Verrelst et al., 2015; Wainwright et al., 2014)

First-order sensitivity index $S_i$ represents the proportion of output variance that can be attributed solely to variations in a single input parameter $X_i$, assuming all other parameters remain unchanged (Song et al., 2012):

$$S_i = \frac{V_{X_i}(E_{\sim i}(Y|X_i))}{VY} \quad (5)$$

In contrast, the total sensitivity index $ST_i$ accounts for the entire contribution of $X_i$ to output variance, including all its interaction effects with other parameters:

https://doi.org/10.5194/egusphere-2025-6076
Preprint. Discussion started: 4 February 2026


$$ST_i = S_i + \sum_{j \neq i} S_{ij} + \sum_{j \neq i, k \neq i, j<k} S_{ijk} + \cdots \quad (6)$$

The Sobol' method provides the most comprehensive sensitivity assessment and is capable of handling highly non-linear and non-monotonic models, but its computational cost is relatively high compared to other methods (Nossent et al., 2011).

## 2.5 Experimental Scheme and Design

The study selected nine key carbon-water cycle variables as model output indicators: (1) carbon flux variables, including Gross Primary Productivity (GPP), Net Ecosystem Exchange (NEE), Soil Carbon Flux (Soil C Flux); (2) hydrological and structural variables, including Leaf Area Index (LAI), and Actual Evapotranspiration (AET); and (3) carbon pool variables, including Vegetation Carbon (Veg C), Litter Carbon (Litter C), Soil Carbon (Soil C), and Total Carbon (Total C).

To systematically evaluate the performance of different sensitivity analysis methods and to investigate the influence of various types of model parameters on carbon-water cycle simulations, a comprehensive experimental framework was designed. First, the 39 parameters were divided into two categories: 19 parameters related to plant physiological processes (hard-coded in the source code), and 20 parameters related to PFT constitution. Second, each parameter group was analyzed independently using three sensitivity analysis methods. Third, to capture the potential interactions across parameter categories and evaluate their joint influence on model outputs, a combined sensitivity analysis was conducted using all 39 parameters. The specific experimental design is summarized in Table 2.

Table 2. Experimental Design Scheme

| **Parameter Category** | **Number of Parameter Sets** | **Number of Parameter Sets** | | |
|---|---|---|---|---|
| | | Morris | eFast | Sobol’ |
| Physiological processes | 19 | 200 | 9899 | 10240 |
| PFT parameters | 20 | 200 | 9940 | 10752 |
| Physiological + PFT | 39 | 400 | 9711 | 10240 |

The generation of parameter sets (shown in Table 2) was guided by the specific requirements of each method. As described in Section 2.4, the Morris method uses a specific One-Factor-at-a-

https://doi.org/10.5194/egusphere-2025-6076
Preprint. Discussion started: 4 February 2026


Time trajectory design, the eFAST method generates sample sets based on sinusoidal functions, and the Sobol' method combinations were generated using standard Monte Carlo sampling.

For the eFAST and Sobol' methods, this resulted in approximately 10,000 parameter combinations, which is sufficient to ensure robust and comprehensive variance decomposition. To improve computational efficiency, parameter updating and model execution for all analyses were fully automated and parallelized using Python process pools.

## 2.6 Data Processing and Statistical Methods

### 2.6.1 Sensitivity Index Calculation and Standardization

To ensure comparability of sensitivity analysis results across methods and target variables, a standardized processing workflow was employed. First, for each parameter, raw sensitivity indices were averaged across the 13 study sites—specifically, the mean of elementary effects ($\mu$) for the Morris method, and the total sensitivity index ($ST_i$) for eFAST and Sobol' methods. In the first stage of standardization, the average sensitivity indices for each parameter $p$, method $m$ and target variable $v$, denoted as $S_{p,m,v}$ were normalized by dividing by the maximum sensitivity value for the corresponding method and variable. This normalization ensured a consistent scale for inter-method comparison. Next, to identify the most influential parameters, a preliminary composite index $\mathrm{Combined}_1$ was computed as the average of the normalized indices from the three methods. Based on $\mathrm{Combined}_1$, a subset of the top-N sensitive parameters was selected for further analysis. These top parameters were then re-standardized across the three methods, and a final comprehensive sensitivity score $\mathrm{Combined}_2$ was calculated by averaging the re-standardized values. This two-stage process enhances interpretability while preserving the relative discriminative power of each sensitivity analysis method.

### 2.6.2 Method Consistency Assessment

To assess the consistency in parameter importance ranking among the Morris, eFAST, and Sobol' methods, two complementary approaches were adopted. Spearman rank correlation analysis ($\rho$) and corresponding $p$-values were used to evaluate monotonic agreement among rankings. Additionally, pairwise linear regression analysis, expessed as $R_B = a + b \times R_A$ were performed to examine systematic differences and relationships in parameter rankings between methods.

https://doi.org/10.5194/egusphere-2025-6076
Preprint. Discussion started: 4 February 2026


#### 2.6.3 Uncertainty Quantification and Spatial Analysis

Model output uncertainty was quantified using the Coefficient of Variation ($CV$), calculated across all parameter samples. To evaluate the consistency of uncertainty estimates between the eFAST and Sobol' methods, both Pearson and Spearman correlation analyses were conducted, along with linear regression modeling. Results were visualized with scatter plots to identify systematic deviations. Spatial patterns of model output uncertainty across sites and vegetation types were further analyzed using Cumulative Distribution Functions (CDFs) and box plots, enabling the identification of regions and vegetation types characterized by highly sensitive or relatively stable model responses.

# 3 Results

## 3.1 Co-dominance of Physiological and PFT Parameters in Model Sensitivity

Our comprehensive sensitivity analysis, conducted using three global methods (Morris, eFAST, Sobol'), reveals a fundamental characteristic of the LPJ-GUESS model: its outputs are not driven by a single class of parameters, but are co-dominated by both core physiological parameters, often hard-coded in the source code, and PFT-specific traits defined in user-facing files. This finding suggests limitations in the common practice of focusing calibration efforts solely on the more accessible PFT parameters (Oberpriller et al., 2022; Peng et al., 2024). A detailed breakdown of sensitivities for physiological versus PFT parameters is provided in Text S2.1 and S2.2.

This co-dominance is illustrated by the two most influential parameters identified across nearly all nine output variables (Fig. 2; see Fig. S1 for full rankings). The highest overall sensitivity was associated with *ALPHA_C3* (intrinsic quantum efficiency of $CO_2$ uptake), a fundamental physiological parameter, which primarily governed carbon flux variables such as GPP and Soil Carbon Flux. Closely ranked was *common_reprfrac* (proportion of NPP allocated to reproduction), a key PFT trait parameter, which exerted dominant control over ecosystem structure and the magnitude of major carbon stocks (Veg C, Litter C, Soil C, and Total C).

This pattern extends beyond the two most influential parameters. The subsequent group of highly sensitive parameters also included a mixture of both parameter types: core physiological parameters like *THETA* (photosynthesis co-limitation shape) and *FRADPAR* (fraction of PAR in

https://doi.org/10.5194/egusphere-2025-6076
Preprint. Discussion started: 4 February 2026


shortwave radiation) were critical for photosynthetic processes, while PFT-specific traits such as *tree_turnover_root* (fine root turnover rate) played a key role in regulating carbon residence time in litter and soil pools.

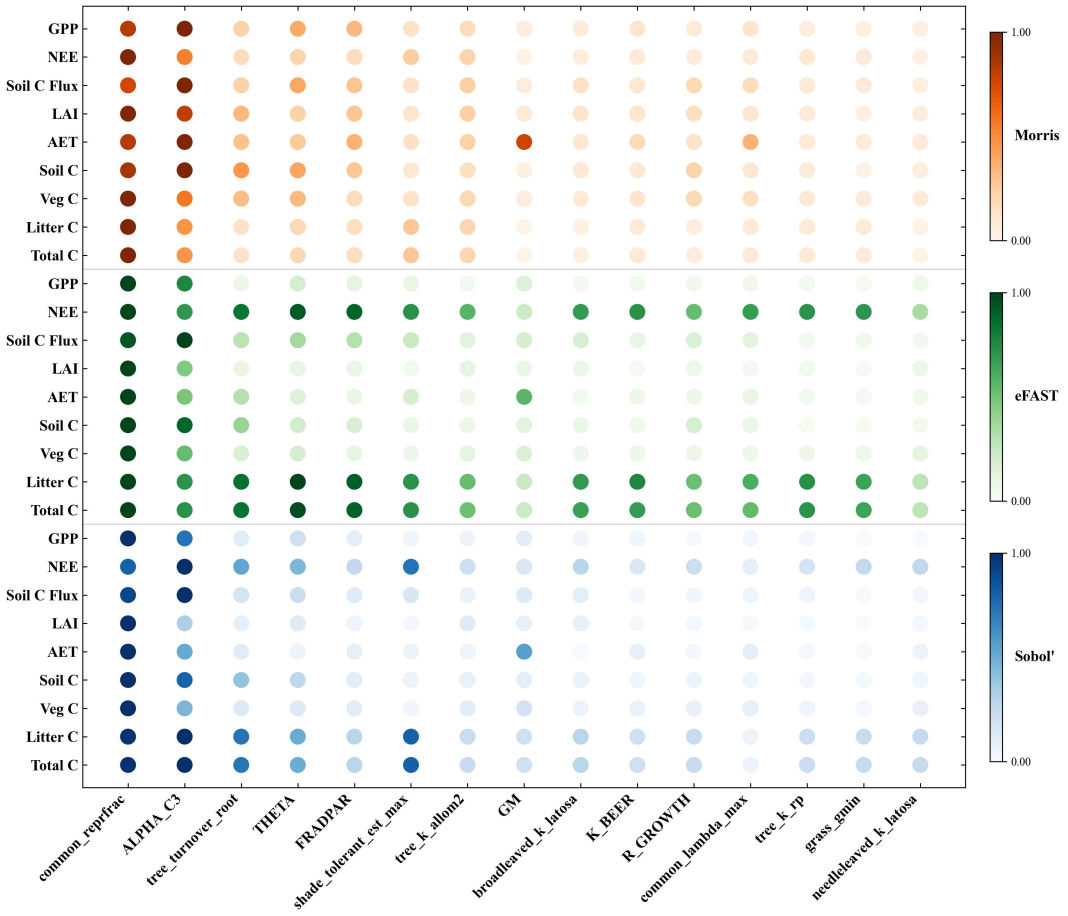


**Fig. 2: Union of the Top 10 Most Sensitive Parameters across All Target Variables for Different Methods**

While all three analysis methods consistently identified this overall hierarchy of control, minor discrepancies in rankings and sensitivity magnitude were observed for less dominant parameters, such as *shade_tolerant_est_max* (Fig. 2). These differences reflect methodological characteristics of individual approaches and underscore the value of applying multiple sensitivity analysis methods in parallel. Moreover, some parameters exhibited process-specific importance:

https://doi.org/10.5194/egusphere-2025-6076
Preprint. Discussion started: 4 February 2026


*GM* (maximum canopy conductance) was particularly influential for AET, whereas the allometric constant *tree_k_allom2* showed a distinct sensitivity signal for LAI.

Overall, these results refine the understanding of parameter influence in LPJ-GUESS. The regulation of carbon-water cycle processes is not solely governed by adjustable PFT traits but is also strongly constrained by core physiological parameters. This co-dependence underscores that efforts to improve model calibration and reduce uncertainty would benefit from a more comprehensive strategy that explicitly considers both parameter types.

### 3.2 Dissecting Parameter Influence: Direct Physiological Control Versus Interactive Allocation Effects

To examine the mechanisms governing the carbon and water cycles, we decomposed the total sensitivity of parameters into direct main effects $S_i$ and higher-order interaction effects $S_{Ti} - S_i$ using the Sobol' and eFAST methods (Fig. 3, Fig. S4-S5). This analysis reveals distinct differences in the parameter control structures of GPP and AET, which are used as representative fluxes.

For GPP, the controlling patterns differ markedly among parameters. The influence of the core physiological constant *ALPHA_C3* (intrinsic quantum efficiency) is dominated by its direct main effect, with only a minor contribution from interaction effects (blue bars, Fig. 3). This suggests that its influence on modeled photosynthetic capacity is largely independent of other parameters. In contrast, the most influential GPP parameter, the PFT trait *common_reprfrac* (NPP allocation to reproduction), displays a substantial contribution from interaction effects, comparable in magnitude to its main effect. This indicates that the impacts of carbon allocation are strongly modulated by interactions with other parameters governing vegetation growth and turnover.

In contrast, the sensitivity of AET is dominated by interaction effects. For all key controlling parameters—including *common_reprfrac*, *ALPHA_C3*, and *GM* (maximum canopy conductance)—interaction effects constitute a substantial, and in several cases dominant, portion of their total influence (orange bars, Fig. 3). This underscores that AET is not governed by individual parameters in isolation, but rather emerges from the combined effects of soil water

https://doi.org/10.5194/egusphere-2025-6076
Preprint. Discussion started: 4 February 2026


availability, canopy properties, and atmospheric demand. Consequently, the influence of any single parameter depends strongly on the overall state of the soil-plant-atmosphere system.

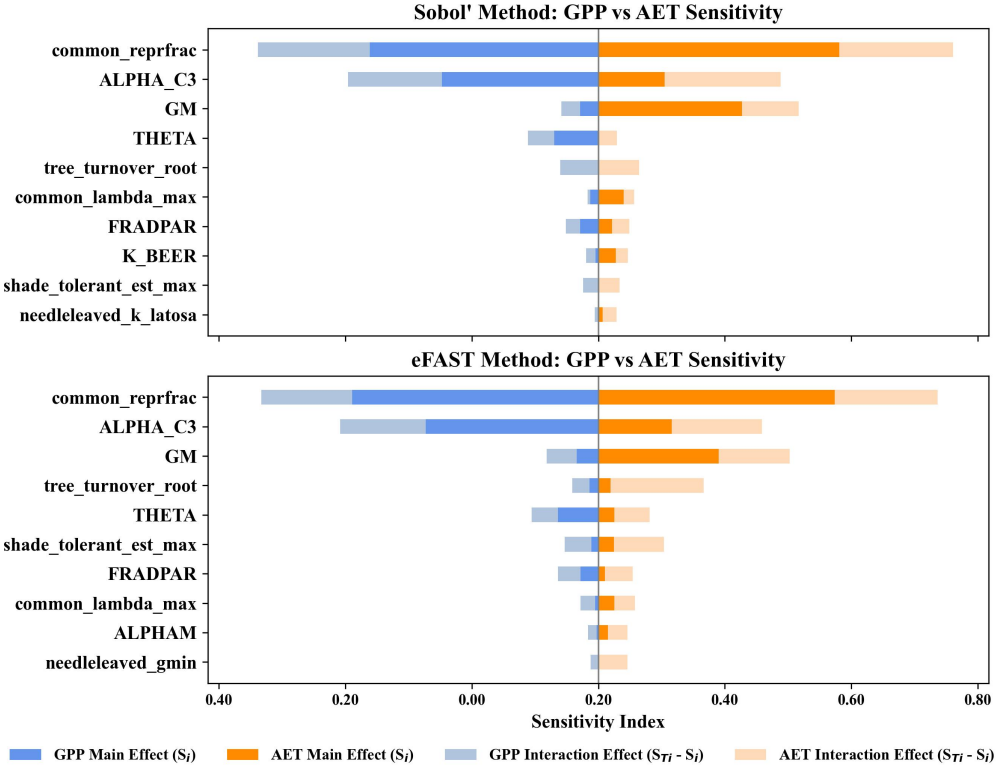


**Fig. 3. Decomposition of parameter sensitivity for GPP and AET into main effects ($S_i$) and interaction effects($S_{Ti} - S_i$) based on the Sobol' method.**

## 3.3 Methodological Consensus and Complementarity in Sensitivity Rankings

To evaluate the robustness of our findings, we assessed the consistency of parameter importance rankings derived from the Morris, eFAST, and Sobol' methods across all nine output variables (Fig. 4). Pairwise comparisons using Spearman rank correlation revealed strong and statistically significant agreement ($p < 0.01$) among all methods, indicating a high degree of consensus in identification of key model controls.

The agreement was particularly notable between the Morris and Sobol' methods, which consistently yielded the strongest correlations, with coefficients ($\rho$) frequently exceeding 0.85 for major outputs such as GPP ($\rho$ = 0.90) and Soil C ($\rho$ = 0.94). The other pairings, while still showing substantial agreement, exhibited greater variability. For instance, the agreement

https://doi.org/10.5194/egusphere-2025-6076
Preprint. Discussion started: 4 February 2026


between eFAST and Sobol' was strong for structural and stock variables (e.g., $\rho$ = 0.76 for LAI), but notably weaker for net fluxes such as NEE ($\rho$ = 0.43). This reduced consistency for NEE is mechanistically plausible, as NEE represents a small residual between two large, opposing fluxes (GPP and ecosystem respiration), which can lead to a more complex and variable sensitivity structure.

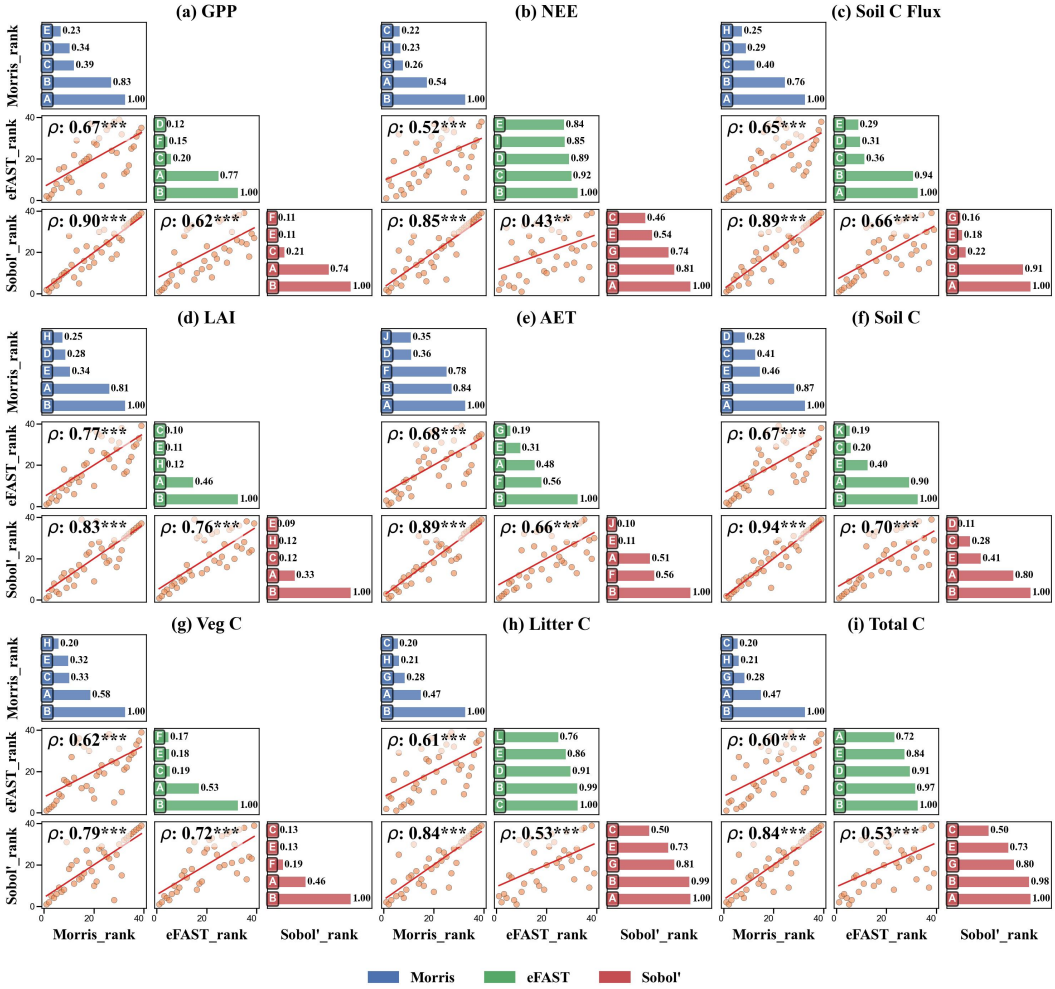


**Fig. 4: Consistency analysis of parameter sensitivity rankings identified by Morris, eFAST, and Sobol' methods across nine output variables. Each of the nine large panels corresponds to a specific model output variable. Within each large panel, the sub-panels compare the sensitivity rankings of the three methods: the diagonal sub-panels display the standardized sensitivity indices for the top-five ranked parameters from each method; the lower-left sub-**

https://doi.org/10.5194/egusphere-2025-6076
Preprint. Discussion started: 4 February 2026


**panels show scatter plots comparing the parameter sensitivity ranks between pairs of methods, annotated with the Spearman's rank correlation coefficient ρ and its statistical significance (*** represents significance < 0.001, ** represents significance < 0.01). The solid line represents the linear regression fit to the ranked scatter points.**

Crucially, this consensus was strongest for the most influential parameters. Across all three methods, *ALPHA_C3* and *common_reprfrac* were consistently identified as the two dominant drivers of GPP. These parameters, along with *tree_turnover_root* and *THETA*, also consistently appeared among the top five ranked parameters for a suite of variables, including Soil C Flux, LAI, and Soil C, with only minor differences in their relative ordering.

Nevertheless, the analysis also highlighted key divergences that underscore the complementarity of the methods. A representative example is *GM* (maximum canopy conductance): while all methods agreed on its top-tier importance for AET, the Morris method assigned it a much lower rank for NEE compared to eFAST and Sobol'. Such discrepancies likely arise from the different mathematical formulations of the methods, particularly in how the parameter space is sampled and how interaction effects are quantified.

In summary, although all three sensitivity analysis methods converge on the primary drivers of the carbon-water cycle in LPJ-GUESS, the subtle variations in their rankings provide additional insight into model behavior. This highlights the benefit of a multi-method framework for a more comprehensive assessment of parameter influence.

## 3.4 Divergent Parameter Controls Across Target Variables

The influence of model parameters varied markedly across the nine output variables, revealing distinct control structures for different components of the carbon-water cycle (Fig. 5).

GPP displayed the most concentrated sensitivity profile. Its response was dominated by a small cohort of photosynthetic parameters—primarily *ALPHA_C3*, followed by *common_reprfrac* and *THETA*. This focused control structure highlights that modeled productivity is largely governed by biochemical efficiency at the leaf level (Fig. 5, a-c).

In contrast, flux and vegetation structure variables exhibited more complex and diversified control structures (Fig. 5, d-f). Soil Carbon Flux sensitivity largely resembled that of GPP, reflecting the tight coupling between carbon input and heterotrophic respiration. NEE, as a net balance, was sensitive to a broader range of physiological and structural parameters. LAI was co-limited by carbon allocation (*common_reprfrac*), productivity (*ALPHA_C3*), and turnover

https://doi.org/10.5194/egusphere-2025-6076
Preprint. Discussion started: 4 February 2026


(*tree_turnover_root*), while AET was particularly sensitive to *GM* (maximum canopy conductance), underscoring the role of stomatal regulation in controlling water fluxes.

The major carbon pools (Vegetation, Litter, and Soil) were governed by a common set of parameters, reflecting shared controls on biomass dynamics. Their sensitivities were co-dominated by production (*ALPHA_C3*), allocation (*common_reprfrac*), and residence time (*tree_turnover_root*). The strong influence of these parameters was most pronounced for Litter C and Total C, where their combined Sobol' sensitivity indices approached 1.0, indicating near-complete model control by these three factors alone (Fig. 5, g-i).

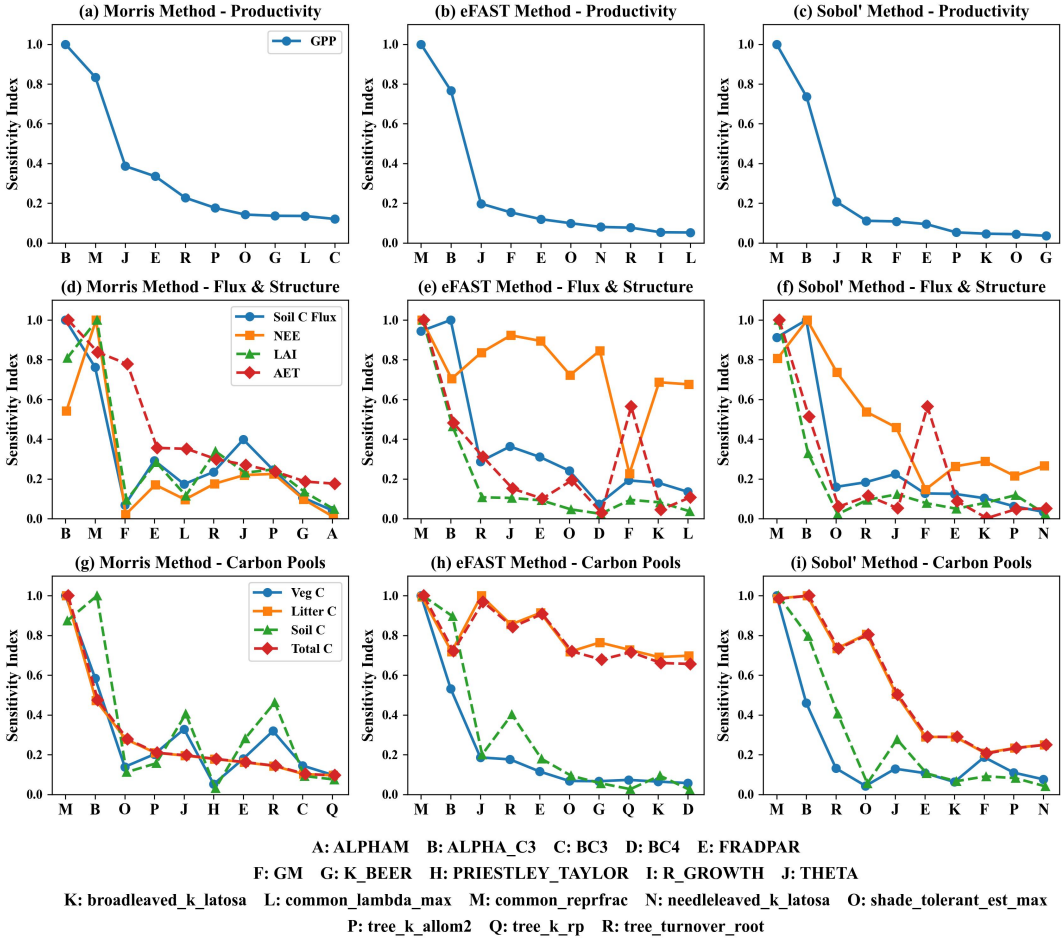


**Fig. 5: Comparison of results from the Morris, eFAST, and Sobol sensitivity analysis methods. Each subplot shows the normalized sensitivity index (Y-axis) of different model parameters (X-axis, letter codes) for three groups of target variables. The rows represent**

https://doi.org/10.5194/egusphere-2025-6076
Preprint. Discussion started: 4 February 2026


**the variable groups of Productivity, Flux & Structure, and Carbon Pools, respectively; the columns correspond to the three analysis methods.**

In summary, different groups of variables are governed by a distinct set of controlling parameters. Productivity is primarily influenced by a small number of photosynthetic inputs, fluxes and vegetation structure by a wider and more complex set of interacting factors, and carbon stocks by the combined effects of production, allocation, and turnover. These findings demonstrate that parameterization and calibration strategies should be aligned with the specific processes of interest, as parameter sets optimized for one component of the system may not perform equivalently for others.

## 3.5 Spatial Heterogeneity of Parameter Controls Across Ecosystems

Parameter sensitivities exhibited pronounced spatial heterogeneity across China's diverse vegetation types, revealing distinct control structures between resource-rich and resource-limited ecosystems (based on eFAST results; Fig. 6).

In humid forest ecosystems (e.g., DBF, EBF, CNV), model behavior was primarily governed by parameters related to physiological efficiency and biomass turnover. GPP sensitivity was highest for *ALPHA_C3*, while AET was most sensitive to stomatal regulation via *GM*. The large carbon pools in these systems, particularly Litter C and Soil C, were strongly controlled by *tree_turnover_root*, reflecting the dominant role of woody biomass turnover in regulating detritus input and long-term carbon storage. Together, these patterns indicate that carbon and water fluxes in humid forests are predominantly controlled by physiological processes operating under relatively favorable resource conditions.

Conversely, arid and semi-arid ecosystems (e.g., BSV, GSL) displayed a distinctly different sensitivity structure, characterized by a stronger influence of resource allocation and use efficiency. The PFT trait *common_reprfrac* (carbon allocation to reproduction) emerged as a key controlling parameter for GPP and LAI and also exerted a strong influence on AET. This suggests that under conditions of severe water limitation, canopy structure, as shaped by carbon allocation strategies, can exert a greater control over water loss in addition to direct stomatal regulation. Furthermore, the net carbon balance (NEE) in these sensitive systems showed high sensitivity to photosynthetic (*ALPHA_C3, BC3*) and radiation-use (*FRADPAR*) parameters, indicating that relatively small changes in carbon assimilation efficiency can substantially affect whether the ecosystem functions as a net carbon sink or source.

https://doi.org/10.5194/egusphere-2025-6076
Preprint. Discussion started: 4 February 2026


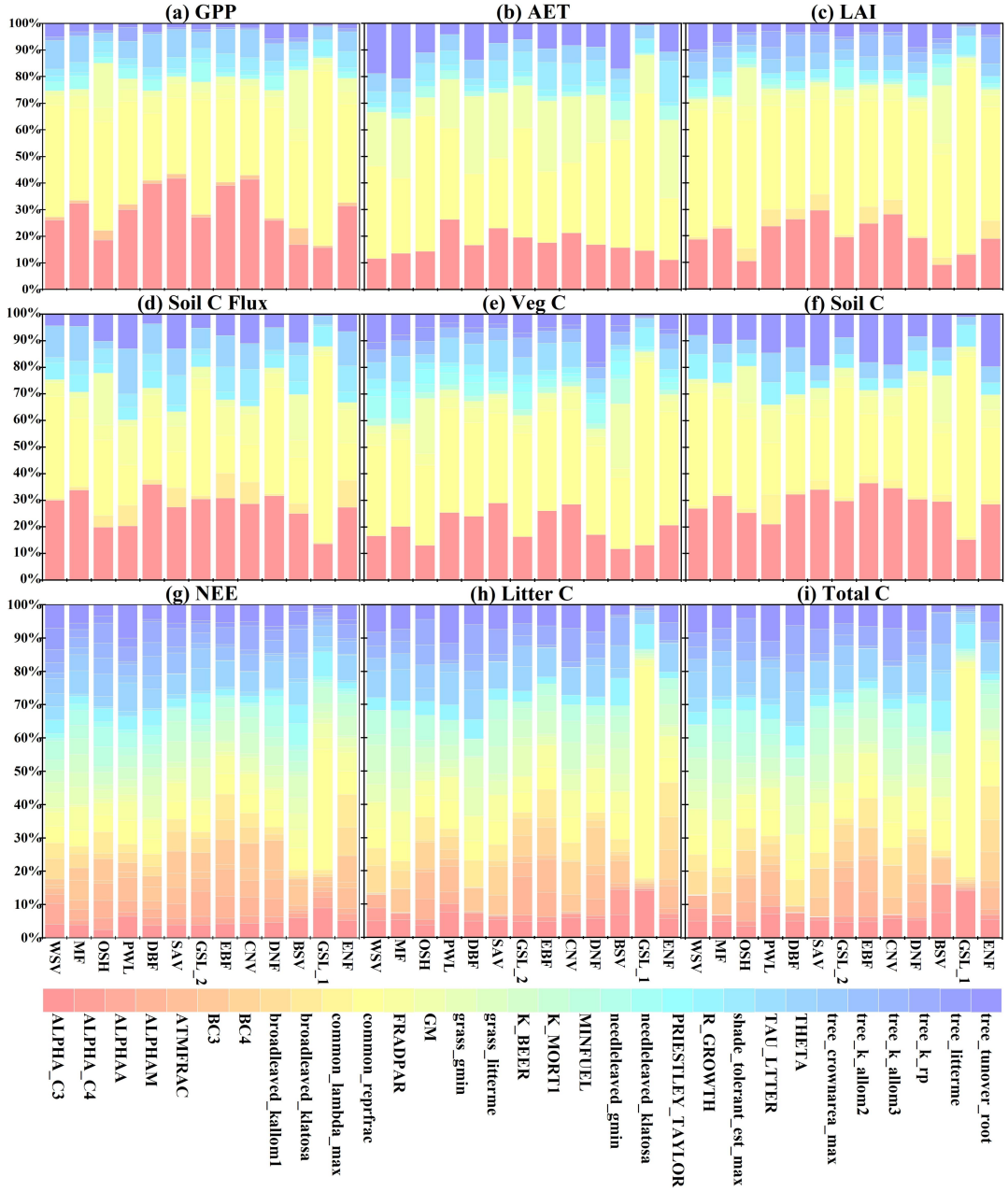


**Fig. 6: Spatial heterogeneity of parameter sensitivity across different vegetation types. Each of the nine panels corresponds to a specific output variable (e.g., GPP, AET). Within each panel, the x-axis represents the 13 different study sites. Each vertical bar is a stacked bar chart, illustrating the relative contribution of the most sensitive parameters (listed in the bottom legend) for that specific site. The color of each segment corresponds to a parameter, and its height represents that parameter's proportional contribution to the total**

https://doi.org/10.5194/egusphere-2025-6076
Preprint. Discussion started: 4 February 2026


**sensitivity (based on the eFAST method). Therefore, within a single panel, significant variation in the color composition across the site bars indicates that the key controlling parameters for that output variable differ greatly between locations. Conversely, similarity in color composition suggests spatial consistency in the controlling parameters.**

In summary, parameter sensitivities are strongly contingent on the ecosystem context. Humid forests are primarily controlled by parameters of physiological process rates and biomass turnover. In contrast, arid systems are more sensitive to parameters governing the strategic allocation of scarce resources. This substantial spatial heterogeneity underscores that uniform parameterization strategies are insufficient. Accurate regional and global modeling therefore require ecosystem-specific calibration strategies to capture the diverse responses of terrestrial ecosystems to environmental change.

## 3.6 Impact of Parameter Uncertainty on Model Output

Following the identification of sensitive parameters, this section investigates how the inherent uncertainty (i.e., variability within their prescribed ranges) of these parameters collectively propagates to affect the overall uncertainty and range of simulated values for key model output variables. Furthermore, it examines whether the magnitude and spatial characteristics of this output uncertainty vary across vegetation types and geographic regions.

### 3.6.1 Consistency of Uncertainty Quantification

To ensure the robustness of our uncertainty assessment, we compared the output Coefficient of Variation (*CV*) derived from both the Sobol' and eFAST methods. The two methods yielded nearly identical uncertainty estimates across all nine output variables (Fig. 7). This high consistency is demonstrated by strong Pearson correlations ($r > 0.97$ for all variables), scatter plots where data points for all vegetation types cluster tightly along the 1:1 line, and regression models with slopes approaching 1.0 and intercepts near zero. These results indicate that both methods provide consistent and comparable quantifications of output uncertainty, supporting the subsequent spatial analysis.

https://doi.org/10.5194/egusphere-2025-6076
Preprint. Discussion started: 4 February 2026


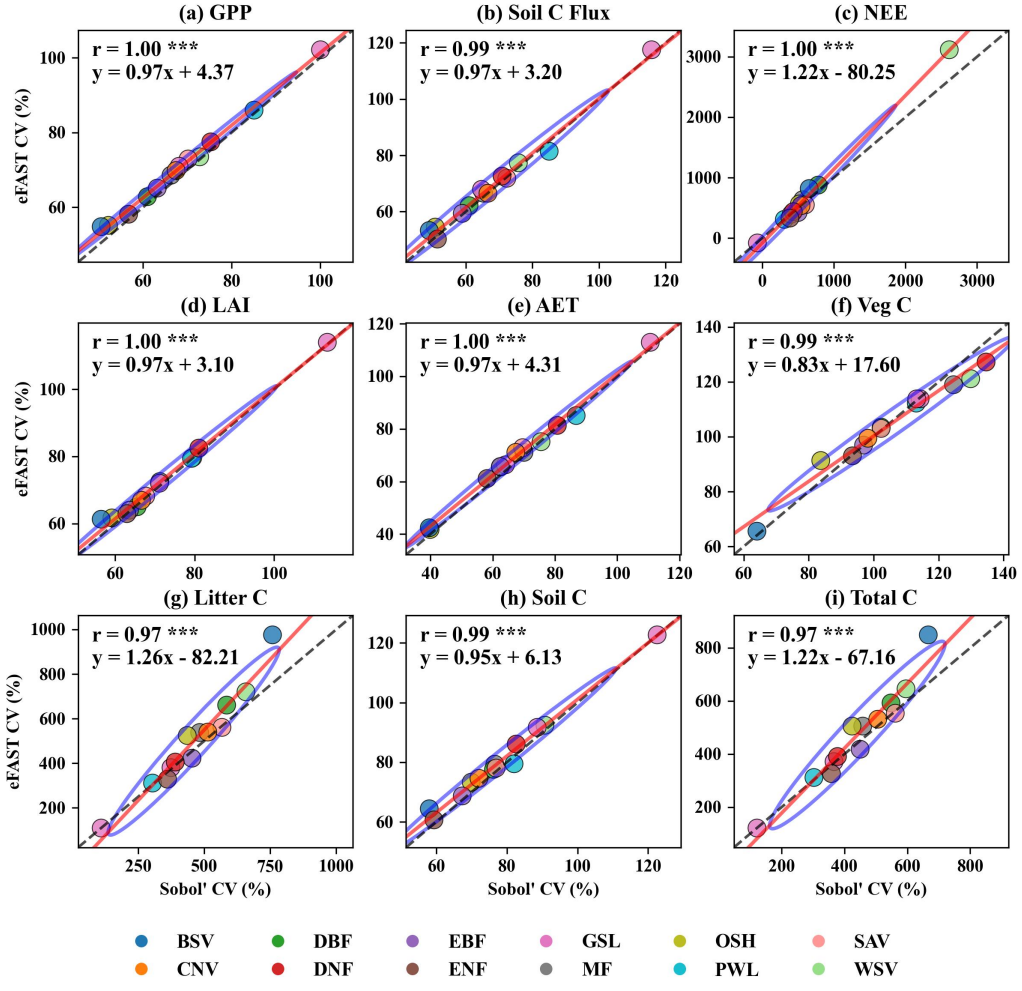


**Fig. 7: Uncertainty Assessment Using Sobol' and eFAST Methods**

### 3.6.2 Opposing Gradients of Productivity and Uncertainty

The propagation of parameter uncertainty into model outputs revealed strong and opposing spatial gradients across China. Using GPP as an illustrative example (Fig. 8), mean productivity increased systematically from the arid northwest to the humid southeast. Conversely, the relative uncertainty of simulated GPP, expressed as *CV*, showed an opposite pattern, with the highest values (*CV* > 80%) occurring in the driest and least productive regions and the lowest values (*CV*

https://doi.org/10.5194/egusphere-2025-6076
Preprint. Discussion started: 4 February 2026


497 < 60%) in the most productive forest areas.

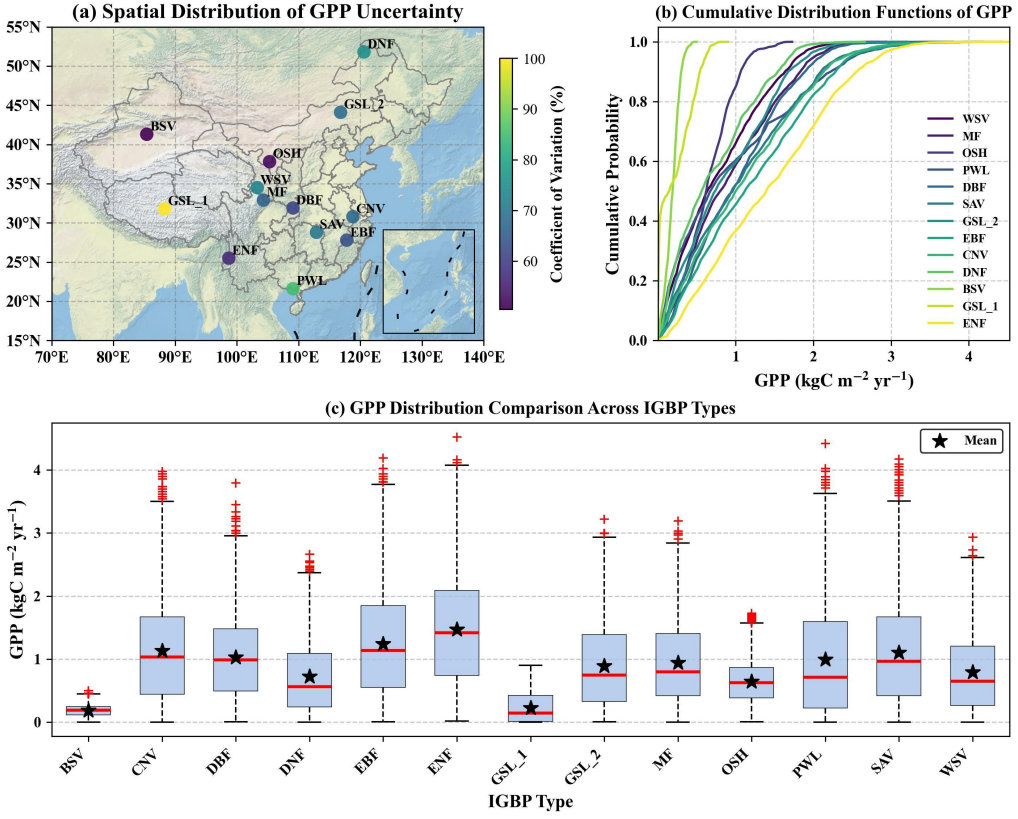


498

499 **Fig. 8: Spatial Distribution Pattern of GPP Uncertainty Across Different Sites**

500 Critically, this analysis uncovers a clear contrast between relative and absolute uncertainty
501 (Fig. 8b, 8c). In the arid northwest, high relative uncertainty indicates strong sensitivity of
502 modeled GPP to parameter variability, but the low baseline productivity results in a relatively
503 small absolute range of simulated values (narrow box plots). In contrast, in the humid southeast,
504 relative uncertainty is lower, yet the high baseline productivity causes even modest relative
505 uncertainty to translate into a large absolute range of simulated GPP (wide box plots), which has
506 important implications for regional carbon budget estimation. This contrast between relative
507 uncertainty in low-productivity regions and absolute uncertainty in high-productivity regions is
508 not unique to LPJ-GUESS, but likely represents a broader challenge for land surface models,
509 including those used in TRENDY and CMIP6 intercomparisons. Similar spatial patterns were
510 also observed for other variables, such as LAI and AET.

https://doi.org/10.5194/egusphere-2025-6076
Preprint. Discussion started: 4 February 2026


These findings underscore that effective uncertainty management requires region-specific strategies. In resource-limited regions, reducing relative uncertainty depends primarily on improving constraints on sensitive parameters. In productive regions, the key challenge lies in constraining the absolute uncertainty of large fluxes, even when relative uncertainty is low, in order to support reliable carbon accounting.

# 4 Discussion

## 4.1 The Core Mechanisms of Model Control: From Parameter Co-dominance to Spatial Divergence

Our multi-method sensitivity analysis, whose robustness is supported by the strong consensus among the Morris, eFAST, and Sobol' methods for top-ranking parameters (Section 3.3), reveals a clear hierarchical and spatially contingent architecture of model control. At a broad level, model behavior is not governed by a single process, but reflects the combined influence of photosynthetic efficiency, carbon allocation strategies, and biomass turnover rates. The relative importance of these processes is not static, but varies systematically across climate gradients, consistent with differences in dominant ecological constraints observed in natural ecosystems (Baral et al., 2014; Liu et al., 2022).

The dominant influence of photosynthetic efficiency—primarily represented by the *ALPHA_C3* parameter—reinforces its role as the ultimate driver of carbon influx into the ecosystem. This aligns with fundamental ecological theory, in which the efficiency of light-use conversion constrains GPP (Farquhar et al., 1980; Thevasundaram et al., 2022). In the model, this control is largely expressed through direct effects, as indicated by the decomposition of main and interaction sensitivities (Section 3.2). However, what happens to this carbon post-assimilation is equally critical. The high sensitivity associated with *common_reprfrac* (carbon allocation) and *tree_turnover_root* (biomass turnover) underscores that patterns of carbon investment among plant tissues and the residence time of biomass exert substantial influence on long-term carbon storage, vegetation structure, and net ecosystem balance (Dong et al., 2024; Wang et al., 2024). This finding suggests that photosynthesis alone is insufficient to explain ecosystem carbon dynamics, and that allocation and turnover represent critical controls on the persistence and distribution of assimilated carbon (Camargo et al., 2023; Kengdo et al., 2023; Zandi et al., 2023).

https://doi.org/10.5194/egusphere-2025-6076
Preprint. Discussion started: 4 February 2026


Crucially, the dominance of these controlling processes is spatially contingent, leading to distinct sensitivity patterns across environments gradients (Pappas et al., 2013). In humid, productive forest ecosystems, model sensitivity is primarily driven by parameters of physiological efficiency. Here, with water being less of a limiting factor, simulated ecosystems operate closer to their maximum photosynthetic potential, making it highly sensitive to *ALPHA_C3*. Furthermore, in structurally complex forest canopies, parameters related to regeneration and light competition (e.g., *shade_tolerant_est_max*) also emerge as influential, while large carbon stocks are primarily regulated by the slow turnover of woody biomass (*tree_turnover_root*). This pattern reflects a system in which intrinsic growth rates competition and biomass persistence play central roles (Bergkvist et al., 2023; Kühn et al., 2021; Pugh et al., 2019).

In contrast, model control shifts towards parameters associated with resource acquisition and allocation in arid and semi-arid ecosystems (Asargew et al., 2024; Lv et al., 2024). In these water-limited environments, survival under stress becomes more influential than maximizing productivity. Consequently, *GM* (stomatal conductance) and *common_reprfrac* (allocation) exert strong control, including for fluxes like AET. This pattern indicates that, within the model framework, conservative water use and allocation strategies play a greater role than photosynthetic capacity alone in regulating ecosystem function under dry conditions (Liu et al., 2022). The heightened sensitivity of NEE to a wider array of parameters in these arid sites further illustrates their inherent sensitivity, where small perturbations in any number of processes can shift the system from a net sink to a source (Liang et al., 2024; Mitchell et al., 2000). These spatially divergent sensitivity patterns suggest that effective model parameterization should reflect contrasting ecological constraints across environments. However, it is important to note that these interpretations are based on the internal logic of LPJ-GUESS. In the absence of systematic validation against site-level observations (e.g., eddy covariance data), these findings should be viewed as model-dependent insights into potential dominant controls rather than direct confirmation of ecosystem mechanisms. Nevertheless, the alignment of these sensitivity patterns with general ecological theory supports the plausibility of the model's representation of key controlling processes.

https://doi.org/10.5194/egusphere-2025-6076
Preprint. Discussion started: 4 February 2026


## 4.2 Rethinking Model Uncertainty: From Spatial Patterns to an Inherent Tradeoff

The propagation of parameter uncertainty through the LPJ-GUESS model is not random but instead follows a clear spatial logic that mirrors the hydro-thermal gradients across China. Our results show that the highest relative uncertainty (*CV*) consistently occurs in the arid and semi-arid ecosystems of the northwest. This pattern is a direct consequence of the mechanisms discussed in the previous section: these water-stressed systems are critically sensitive to a few dominant parameters controlling resource use and allocation (e.g., *GM, common_reprfrac*). As a result, the model behavior in these regions is highly variable, where small parameter perturbations can lead to large proportional changes in outputs (Liang et al., 2024). Conversely, the humid and highly productive ecosystems in the southeast exhibit the lowest relative uncertainty, suggesting a buffering effect where a more complex web of interacting, non-dominant parameters creates a more robust and stable system response (Bello et al., 2021; Gómez-Gras et al., 2021).

However, a deeper analysis reveals a fundamental—and critically important—tradeoff between relative and absolute uncertainty. The low relative uncertainty in humid forests should not be misconstrued as a lack of modeling challenge. While the model is robust in these regions (low *CV*), the high baseline productivity and carbon fluxes imply that even small relative error translates into substantial absolute uncertainty in terms of actual carbon mass (kgC $m^{-2}$ $yr^{-1}$). For example, a 5% uncertainty associated with a GPP of 1.5 kgC $m^{-2}$ $yr^{-1}$ represents a much larger quantity of unknown carbon than a 20% uncertainty associated with a GPP of 0.2 kgC $m^{-2}$ $yr^{-1}$ in an arid ecosystem.

This tradeoff redefines the nature of model risk across different regions. In arid ecosystems, the primary risk is relative instability: inaccurate parameterization can lead to qualitatively incorrect predictions of ecosystem functioning (e.g., predicting a sink when it is a source). In humid, productive ecosystems, the risk shifts to quantitative magnitude. Even for a well-calibrated and structurally robust model, the resulting absolute uncertainty range can be enough to substantially impact regional or global carbon budget calculations. This finding demonstrates that managing and interpreting model uncertainty requires ecosystem-specific perspectives, moving beyond reliance on a single metric like *CV* and toward an integrated understanding of

https://doi.org/10.5194/egusphere-2025-6076
Preprint. Discussion started: 4 February 2026


both relative sensitivity and absolute uncertainty across contrasting environmental contexts (Ma et al., 2022b).

### 4.3 Outlook: From Model Optimization to Future Directions

The findings of this study provide a scientific basis for improving the application and parameterization of DGVMs such as LPJ-GUESS. Our results argue against one-size-fits-all calibration strategies and instead support the adoption of more nuanced, targeted approaches. First, model calibration should follow a hierarchical strategy. Priority should be given to globally sensitive parameters that govern core ecosystem processes (e.g., *ALPHA_C3*, *common_reprfrac*), followed by targeted tuning for specific variables or regions where additional sensitivity emerges (Gong & Duan, 2017; Yu et al., 2022). Second, calibration must be spatially explicit. The distinctly different sensitivity signatures observed between humid and arid ecosystems clearly indicate that region-specific parameter sets are required to reflect their contrasting environmental constraints and limiting factors (Ma et al., 2022a). Third, given the tradeoff between relative and absolute uncertainty, a multi-objective framework that simultaneously constrains both fluxes (e.g., GPP) and stocks (e.g., Soil C) is essential for robust carbon accounting (Arbolino et al., 2021; Rahimi et al., 2023).

Despite the comprehensive nature of our analysis, this study has limitations that define the scope for future research. First, this study relies exclusively on model simulations to diagnose the intrinsic behavior of LPJ-GUESS. While we acknowledge the lack of systematic validation against observational benchmarks (e.g., FLUXNET data), this was a deliberate methodological choice. Conducting GSA prior to calibration is critical to avoid equifinality—getting acceptable model performance for the wrong reasons. By mapping the model's unconstrained sensitivity first, we identify exactly which parameters require observational constraints, thus serving as a necessary prerequisite for robust, data-driven calibration in future works.

Second, we focused primarily on parameter uncertainty, while other important uncertainty sources, such as errors in climate forcing data and model structural assumptions, were not explicitly quantified. Future research should therefore move towards an integrated assessment that combines parameter, driver, and structural uncertainties, aiming to enhance model credibility within the context of global efforts such as TRENDY and CMIP6.

https://doi.org/10.5194/egusphere-2025-6076
Preprint. Discussion started: 4 February 2026


Third, and importantly, our sensitivity analysis assumed parameter independence. However, in reality, many physiological parameters often exhibit covariance due to underlying biological trade-offs (e.g., between photosynthetic capacity and leaf nitrogen). Ignoring these correlations may overestimate the effective parameter space and the resulting model sensitivity. Future studies should aim to incorporate parameter correlation matrices into the sampling design to provide a more constrained estimate of uncertainty.

These limitations directly inform our vision for the future of ecosystem modeling. An important next step is to extend this analysis to a spatially continuous grid, allowing for the creation of national-scale sensitivity maps that explicitly capture geographic variability in model behavior (Ma et al., 2022a). In parallel, a key priority should be given to fully integrated uncertainty frameworks that explicitly address the interplay of parameter, structural, and driver uncertainties (Oberpriller et al., 2022). Moreover, the increasing availability of multi-source data streams (e.g., eddy covariance, remote sensing, soil inventories) offers unprecedented opportunities to validate sensitivity analyses and to develop more advanced data assimilation schemes (Tao et al., 2020). Finally, exploring the dynamic behavior of these parameter sensitivities under future climate change scenarios, potentially aided by machine learning techniques, will be crucial for enhancing the predictive power of terrestrial ecosystem models in a rapidly changing world (Buster et al., 2024; Gou & Soja, 2024; Hagenauer & Helbich, 2022; Jung & Lee, 2021; Love et al., 2024; Reichstein et al., 2019).

# 5 Conclusions

This study provides a comprehensive assessment of parameter controls and uncertainty propagation in the LPJ-GUESS model across China's diverse ecosystems. By integrating three complementary sensitivity analysis methods, we reveal a clear, hierarchical architecture of model control. The simulated carbon-water cycle is co-dominated by a few key parameters governing photosynthetic efficiency (*ALPHA_C3*), carbon allocation (*common_reprfrac*), and biomass turnover. Critically, the dominance of these controls is spatially contingent, shifting from a system governed by physiological efficiency in humid forests to systems constrained by strategic resource allocation and water use in arid and semi-arid ecosystems.

Furthermore, our analysis uncovers a fundamental tradeoff in how parameter uncertainty propagates. Arid ecosystems exhibit the highest relative uncertainty, yet their low productivity

https://doi.org/10.5194/egusphere-2025-6076
Preprint. Discussion started: 4 February 2026


results in a comparatively small absolute uncertainty range. Conversely, humid and highly productive ecosystems, despite showing greater robustness and low relative uncertainty, are associated with the largest absolute uncertainty in carbon fluxes. This finding highlights distinct modeling challenges across different environments.

Collectively, these findings support a move away from one-size-fits-all parameterization towards hierarchical, spatially-explicit, and multi-objective optimization strategies. Future research should focus on extending these analyses to continuous grids and integrating multiple sources of uncertainty (e.g., driver data, model structure) to enhance the predictive reliability of terrestrial biosphere models under ongoing and future environmental change.

https://doi.org/10.5194/egusphere-2025-6076
Preprint. Discussion started: 4 February 2026


## CRediT authorship contribution statement

**Fulai Feng:** Conceptualization, Validation, Formal analysis, Writing – original draft, Writing – review & editing, Visualization. **Jianwu Yan:** Writing – review & editing, Methodology, Funding acquisition, Conceptualization.**Wei Liang:** Writing review & editing. **Xiaohong Liu:** Writing review & editing. **Bo Liu:** Writing review & editing. **Xiaoru Liang:** Visualization, Writing review & editing. **Jia Wei:** Writing review & editing. **Yangcan Bao:** Visualization, Writing review & editing.

## Acknowledgments

This work was performed with financial support from National Natural Science Foundation of China (42330501, 42071144), and in part by Natural Science Basic Research Plan of Shaanxi Province (2023JC-YB-275).

## Conflict of Interest

The authors declare that they have no competing interests.

## Data Availability Statement

The LPJ-GUESS model (version 4.1.1), an open-access software available under the Mozilla Public License v. 2.0, was used to generate the results of this study and can be downloaded from https://zenodo.org/records/8065737 (Nord et al., 2021). Climate data (temperature, precipitation, and shortwave radiation) are available from https://cds.climate.copernicus.eu/datasets/reanalysis-era5-land-monthly-means?tab=download (Copernicus Climate Change Service, 2019). Soil data were obtained from https://data.tpdc.ac.cn/en/data/46ddd893-3b2b-4bb3-b9e6-b043f3c5c3a2 (Shi et al., 2025). Land cover data for site selection were based on the NASA MODIS MCD12C1 product (2001-2023), downloaded from https://e4ftl01.cr.usgs.gov/MOTA/MCD12C1.061/ (Friedl & Sulla-Menashe, 2022). Carbon dioxide data were obtained from the NOAA Global Monitoring Laboratory (https://gml.noaa.gov/ccgg/trends/) (Lan et al., 2023), and nitrogen deposition data can be downloaded from https://data.isimip.org/search/product/InputData/subcategory/n-deposition/ (Lamarque et al., 2013).

https://doi.org/10.5194/egusphere-2025-6076
Preprint. Discussion started: 4 February 2026


## References

Arbolino, R., Boffardi, R., De Simone, L., and Ioppolo, G.: Multi-objective optimization technique: A novel approach in tourism sustainability planning, J. Environ. Manage., 285, 112016, https://doi.org/10.1016/j.jenvman.2021.112016, 2021.

Asargew, M. F., Masutomi, Y., Kobayashi, K., and Aono, M.: Water stress changes the relationship between photosynthesis and stomatal conductance, Sci. Total Environ., 907, 167886, https://doi.org/10.1016/j.scitotenv.2023.167886, 2024.

Baral, B. R., Kuyper, T. W., and Van Groenigen, J. W.: Liebig's law of the minimum applied to a greenhouse gas: Alleviation of P-limitation reduces soil N2O emission, Plant Soil, 374, 539–548, https://doi.org/10.1007/s11104-013-1913-8, 2014.

Bello, F. de, Lavorel, S., Hallett, L. M., Valencia, E., Garnier, E., Roscher, C., Conti, L., Galland, T., Goberna, M., Májeková, M., Montesinos-Navarro, A., Pausas, J. G., Verdú, M., E-Vojtkó, A., Götzenberger, L., and Lepš, J.: Functional trait effects on ecosystem stability: Assembling the jigsaw puzzle, Trends Ecol. Evol., 36, 822–836, https://doi.org/10.1016/j.tree.2021.05.001, 2021.

Bergkvist, J., Lagergren, F., Linderson, M.-L. F., Miller, P., Lindeskog, M., and Jönsson, A. M.: Modelling managed forest ecosystems in Sweden: An evaluation from the stand to the regional scale, Ecol. Model., 477, 110253, https://doi.org/10.1016/j.ecolmodel.2022.110253, 2023.

Bonan, G. B., Levis, S., Sitch, S., Vertenstein, M., and Oleson, K. W.: A dynamic global vegetation model for use with climate models: concepts and description of simulated vegetation dynamics, Glob. Change Biol., 9, 1543–1566, https://doi.org/10.1046/j.1365-2486.2003.00681.x, 2003.

Buster, G., Benton, B. N., Glaws, A., and King, R. N.: High-resolution meteorology with climate change impacts from global climate model data using generative machine learning, Nat. Energy, https://doi.org/10.1038/s41560-024-01507-9, 2024.

Camargo, A. P., de Souza, R. S. C., Jose, J., Gerhardt, I. R., Dante, R. A., Mukherjee, S., Huntemann, M., Kyrpides, N. C., Carazzolle, M. F., and Arruda, P.: Plant microbiomes harbor potential to promote nutrient turnover in impoverished substrates of a brazilian biodiversity hotspot, ISME J, 17, 354–370, https://doi.org/10.1038/s41396-022-01345-1, 2023.

Chen, S.-P. and Hu, Z.-M.: Ecosystem carbon and water fluxes in ecological vulnerable areas in China, Chin. J. Plant Ecol., 46, 1433–1436, https://doi.org/10.17521/cjpe.2022.0404, 2022.

Collatz, G. J., Berry, J. A., Farquhar, G. D., and Pierce, J.: The relationship between the rubisco reaction mechanism and models of photosynthesis, Plant Cell Environ., 13, 219–225, https://doi.org/10.1111/j.1365-3040.1990.tb01306.x, 1990.

Copernicus Climate Change Service: ERA5-land monthly averaged data from 1950 to present, https://doi.org/10.24381/CDS.68D2BB30, 2019.

https://doi.org/10.5194/egusphere-2025-6076
Preprint. Discussion started: 4 February 2026


734 Dong, R., Li, N., Li, M.-H., Cong, Y., Du, H., Gao, D., and He, H. S.: Carbon allocation in picea
735 jezoensis: Adaptation strategies of a non-treeline species at its upper elevation limit,
736 Forest Ecosystems, 11, 100188, https://doi.org/10.1016/j.fecs.2024.100188, 2024.

737 Ehleringer, J. and Björkman, O.: Quantum yields for $CO_2$ uptake in $C_3$ and $C_4$ plants:
738 Dependence on temperature, $CO_2$ , and $O_2$ concentration, Plant Physiol., 59, 86–90,
739 https://doi.org/10.1104/pp.59.1.86, 1977.

740 Enquist, B. J. and Niklas, K. J.: Global allocation rules for patterns of biomass partitioning in
741 seed plants, Science, 295, 1517–1520, https://doi.org/10.1126/science.1066360, 2002.

742 Farquhar, G. D., Von Caemmerer, S., and Berry, J. A.: A biochemical model of photosynthetic
743 CO2 assimilation in leaves of C3 species, Planta, 149, 78–90,
744 https://doi.org/10.1007/BF00386231, 1980.

745 Forster, P. M., Smith, C., Walsh, T., Lamb, W. F., Lamboll, R., Hall, B., Hauser, M., Ribes, A.,
746 Rosen, D., Gillett, N. P., Palmer, M. D., Rogelj, J., von Schuckmann, K., Trewin, B.,
747 Allen, M., Andrew, R., Betts, R. A., Borger, A., Boyer, T., Broersma, J. A., Buontempo,
748 C., Burgess, S., Cagnazzo, C., Cheng, L., Friedlingstein, P., Gettelman, A., Gütschow, J.,
749 Ishii, M., Jenkins, S., Lan, X., Morice, C., Mühle, J., Kadow, C., Kennedy, J., Killick, R.
750 E., Krummel, P. B., Minx, J. C., Myhre, G., Naik, V., Peters, G. P., Pirani, A., Pongratz,
751 J., Schleussner, C.-F., Seneviratne, S. I., Szopa, S., Thorne, P., Kovilakam, M. V. M.,
752 Majamäki, E., Jalkanen, J.-P., van Marle, M., Hoesly, R. M., Rohde, R., Schumacher, D.,
753 van der Werf, G., Vose, R., Zickfeld, K., Zhang, X., Masson-Delmotte, V., and Zhai, P.:
754 Indicators of global climate change 2023: Annual update of key indicators of the state of
755 the climate system and human influence, Earth Syst. Sci. Data, 16, 2625–2658,
756 https://doi.org/10.5194/essd-16-2625-2024, 2024.

757 Friedl, M. and Sulla-Menashe, D.: MODIS/terra+aqua land cover type yearly L3 global 500m
758 SIN grid V061, https://doi.org/10.5067/MODIS/MCD12Q1.061, 2022.

759 Gómez-Gras, D., Linares, C., Dornelas, M., Madin, J. S., Brambilla, V., Ledoux, J., López-
760 Sendino, P., Bensoussan, N., and Garrabou, J.: Climate change transforms the functional
761 identity of mediterranean coralligenous assemblages, Ecol. Lett., 24, 1038–1051,
762 https://doi.org/10.1111/ele.13718, 2021.

763 Gong, W. and Duan, Q.: An adaptive surrogate modeling-based sampling strategy for parameter
764 optimization and distribution estimation (ASMO-PODE), Environ. Modell. Softw., 95,
765 61–75, https://doi.org/10.1016/j.envsoft.2017.05.005, 2017.

766 Gou, J. and Soja, B.: Global high-resolution total water storage anomalies from self-supervised
767 data assimilation using deep learning algorithms, Nat. Water, 2, 139–150,
768 https://doi.org/10.1038/s44221-024-00194-w, 2024.

769 Guan, Q., Tang, J., Feng, L., Olin, S., and Schurgers, G.: Long-term changes of nitrogen
770 leaching and the contributions of terrestrial nutrient sources to lake eutrophication
771 dynamics on the Yangtze Plain of China, Biogeosciences, 20, 1635–1648,
772 https://doi.org/10.5194/bg-20-1635-2023, 2023.

773 Hagenauer, J. and Helbich, M.: A geographically weighted artificial neural network, Int. J. Geogr.
774 Inf. Sci., 36, 215–235, https://doi.org/10.1080/13658816.2021.1871618, 2022.

https://doi.org/10.5194/egusphere-2025-6076
Preprint. Discussion started: 4 February 2026


Hallgren, W. S. and Pitman, A. J.: The uncertainty in simulations by a global biome model (BIOME3) to alternative parameter values, Glob. Change Biol., 6, 483–495, https://doi.org/10.1046/j.1365-2486.2000.00325.x, 2000.

Haxeltine, A. and Prentice, I. C.: A general model for the light-use efficiency of primary production, Funct. Ecol., 10, 551, https://doi.org/10.2307/2390165, 1996.

Hickler, T., Rammig, A., and Werner, C.: Modelling CO2 Impacts on Forest Productivity, Curr Forestry Rep, 1, 69–80, https://doi.org/10.1007/s40725-015-0014-8, 2015.

Jung, Y. and Lee, I.: Optimal design of experiments for optimization-based model calibration using fisher information matrix, Reliab. Eng. Syst. Saf., 216, 107968, https://doi.org/10.1016/j.ress.2021.107968, 2021.

Kengdo, S. K., Ahrens, B., Tian, Y., Heinzle, J., Wanek, W., Schindlbacher, A., and Borken, W.: Increase in carbon input by enhanced fine root turnover in a long-term warmed forest soil, Sci. Total Environ., 855, 158800, https://doi.org/10.1016/j.scitotenv.2022.158800, 2023.

Körner, Ch.: Leaf diffusive conductances in the major vegetation types of the globe, in: Ecophysiology of Photosynthesis, edited by: Schulze, E.-D. and Caldwell, M. M., Springer Berlin Heidelberg, Berlin, Heidelberg, 463–490, https://doi.org/10.1007/978-3-642-79354-7_22, 1995.

Kühn, N., Tovar, C., Carretero, J., Vandvik, V., Enquist, B. J., and Willis, K. J.: Globally important plant functional traits for coping with climate change, Front. Biogeogr., 13, https://doi.org/10.21425/F5FBG53774, 2021.

Lamarque, J.-F., Dentener, F., McConnell, J., Ro, C.-U., Shaw, M., Vet, R., Bergmann, D., Cameron-Smith, P., Dalsoren, S., Doherty, R., Faluvegi, G., Ghan, S. J., Josse, B., Lee, Y. H., MacKenzie, I. A., Plummer, D., Shindell, D. T., Skeie, R. B., Stevenson, D. S., Strode, S., Zeng, G., Curran, M., Dahl-Jensen, D., Das, S., Fritzsche, D., and Nolan, M.: Multi-model mean nitrogen and sulfur deposition from the Atmospheric Chemistry and Climate Model Intercomparison Project (ACCMIP): evaluation of historical and projected future changes, Atmos. Chem. Phys., 13, 7997–8018, https://doi.org/10.5194/acp-13-7997-2013, 2013.

Lan, X., Tans, P., Thoning, K., and NOAA Global Monitoring Laboratory: Trends in globally-averaged CO2 determined from NOAA global monitoring laboratory measurements., https://doi.org/10.15138/9N0H-ZH07, 2023.

Leverenz, J. W.: The effects of illumination sequence, $CO_2$ concentration, temperature and acclimation on the convexity of the photosynthetic light response curve, Physiol. Plant., 74, 332–341, https://doi.org/10.1111/j.1399-3054.1988.tb00639.x, 1988.

Li, Y., Wang, Y., Sun, Y., and Li, J.: Global Sensitivity Analysis of the LPJ Model for Larix olgensis Henry Forests NPP in Jilin Province, China, Forests, 13, 874, https://doi.org/10.3390/f13060874, 2022.

Liang, X., Yan, J., Liang, W., Li, B., Liu, X., Feng, F., and Wei, J.: Ecosystem water limitation shifts driven by soil moisture in the loess plateau, China, Glob. Planet. Change., 243, 104625, https://doi.org/10.1016/j.gloplacha.2024.104625, 2024.

https://doi.org/10.5194/egusphere-2025-6076
Preprint. Discussion started: 4 February 2026


Lindeskog, M., Arneth, A., Bondeau, A., Waha, K., Seaquist, J., Olin, S., and Smith, B.: Implications of accounting for land use in simulations of ecosystem carbon cycling in Africa, Earth Syst. Dynam., 4, 385–407, https://doi.org/10.5194/esd-4-385-2013, 2013.

Lindeskog, M., Smith, B., Lagergren, F., Sycheva, E., Ficko, A., Pretzsch, H., and Rammig, A.: Accounting for forest management in the estimation of forest carbon balance using the dynamic vegetation model LPJ-GUESS (v4.0, r9710): implementation and evaluation of simulations for Europe, Geosci. Model Dev., 14, 6071–6112, https://doi.org/10.5194/gmd-14-6071-2021, 2021.

Liu, C., Li, C., and Li, L.: Climate Warming Benefits Plant Growth but Not Net Carbon Uptake: Simulation of Alaska Tundra and Needle Leaf Forest Using LPJ-GUESS, Land, 13, 632, https://doi.org/10.3390/land13050632, 2024.

Liu, X., Liu, C., Fan, B., Li, L., Tan, B., Jin, Z., Lu, H., and Liu, T.: Spatial responses of ecosystem water-use efficiency to hydrothermal and vegetative gradients in alpine grassland ecosystem in drylands, Ecol. Indic., 141, 109064, https://doi.org/10.1016/j.ecolind.2022.109064, 2022.

Love, R., Milne, G. A., Ajourlou, P., Parang, S., Tarasov, L., and Latychev, K.: A fast surrogate model for 3D earth glacial isostatic adjustment using tensorflow (v2.8.0) artificial neural networks, Geosci. Model Dev., 17, 8535–8551, https://doi.org/10.5194/gmd-17-8535-2024, 2024.

Lv, S., Wang, Z., Yan, B., Liu, H., Han, G., Wang, Z., Li, Z., Wang, Z., Song, X., and Kang, S.: The relationships between structure and function of plant communities in the desert steppe, BMC Plant Biol., 24, 983, https://doi.org/10.1186/s12870-024-05659-4, 2024.

Ma, H., Zhang, K., Ma, C., Wu, X., Wang, C., Zheng, Y., Zhu, G., Yuan, W., and Li, X.: Research progress on parameter sensitivity analysis in ecological and hydrological models of remote sensing, Natl. Remote Sens. Bull., 26, 286–298, https://doi.org/10.11834/jrs.20219089, 2022a.

Ma, R., Xiao, J., Liang, S., Ma, H., He, T., Guo, D., Liu, X., and Lu, H.: Pixel-level parameter optimization of a terrestrial biosphere model for improving estimation of carbon fluxes with an efficient model–data fusion method and satellite-derived LAI and GPP data, Geosci. Model Dev., 15, 6637–6657, https://doi.org/10.5194/gmd-15-6637-2022, 2022b.

Magnani, F., Leonardi, S., Tognetti, R., Grace, J., and Borghetti, M.: Modelling the surface conductance of a broad-leaf canopy: Effects of partial decoupling from the atmosphere, Plant Cell Environ., 21, 867–879, https://doi.org/10.1046/j.1365-3040.1998.00328.x, 1998.

Meentemeyer, V.: Macroclimate and lignin control of litter decomposition rates, Ecology, 59, 465–472, https://doi.org/10.2307/1936576, 1978.

Mitchell, R. J., Auld, M. H. D., Le Duc, M. G., and Robert, M. H.: Ecosystem stability and resilience: A review of their relevance for the conservation management of lowland heaths, Perspect. Plant Ecol. Evol. Syst., 3, 142–160, https://doi.org/10.1078/1433-8319-00009, 2000.

Monteith, J. L.: Accommodation between transpiring vegetation and the convective boundary layer, J. Hydrol., 166, 251–263, https://doi.org/10.1016/0022-1694(94)05086-D, 1995.

https://doi.org/10.5194/egusphere-2025-6076
Preprint. Discussion started: 4 February 2026


Morris, M. D.: Factorial sampling plans for preliminary computational experiments, Technometrics, 33, 161–174, https://doi.org/10.1080/00401706.1991.10484804, 1991.

Nord, J., Anthoni, P., Gregor, K., Gustafson, A., Hantson, S., Lindeskog, M., Meyer, B., Miller, P., Nieradzik, L., Olin, S., Papastefanou, P., Smith, B., Tang, J., Wårlind, D., and Past LPJ-GUESS Contributors: LPJ-GUESS release v4.1.1 model code, , https://doi.org/10.5281/ZENODO.8065736, 2021.

Nossent, J., Elsen, P., and Bauwens, W.: Sobol' sensitivity analysis of a complex environmental model, Environ. Modell. Softw., 26, 1515–1525, https://doi.org/10.1016/j.envsoft.2011.08.010, 2011.

Oberpriller, J., Herschlein, C., Anthoni, P., Arneth, A., Krause, A., Rammig, A., Lindeskog, M., Olin, S., and Hartig, F.: Climate and parameter sensitivity and induced uncertainties in carbon stock projections for European forests (using LPJ-GUESS 4.0), Geosci. Model Dev., 15, 6495–6519, https://doi.org/10.5194/gmd-15-6495-2022, 2022.

Olin, S., Schurgers, G., Lindeskog, M., Wårlind, D., Smith, B., Bodin, P., Holmér, J., and Arneth, A.: Modelling the response of yields and tissue C : N to changes in atmospheric CO<sub>2</sub> and N management in the main wheat regions of western Europe, Biogeosciences, 12, 2489–2515, https://doi.org/10.5194/bg-12-2489-2015, 2015.

Pappas, C., Fatichi, S., Leuzinger, S., Wolf, A., and Burlando, P.: Sensitivity analysis of a process-based ecosystem model: Pinpointing parameterization and structural issues, JGR Biogeosciences, 118, 505–528, https://doi.org/10.1002/jgrg.20035, 2013.

Peng, S., Terrer, C., Smith, B., Ciais, P., Han, Q., Nan, J., Fisher, J. B., Chen, L., Deng, L., and Yu, K.: Carbon restoration potential on global land under water resource constraints, Nat. Water, https://doi.org/10.1038/s44221-024-00323-5, 2024.

Pugh, T. A. M., Lindeskog, M., Smith, B., Poulter, B., Arneth, A., Haverd, V., and Calle, L.: Role of forest regrowth in global carbon sink dynamics, Proc. Natl. Acad. Sci. U.S.A., 116, 4382–4387, https://doi.org/10.1073/pnas.1810512116, 2019.

Rahimi, I., Gandomi, A. H., Chen, F., and Mezura-Montes, E.: A review on constraint handling techniques for population-based algorithms: From single-objective to multi-objective optimization, Arch. Comput. Methods Eng., 30, 2181–2209, https://doi.org/10.1007/s11831-022-09859-9, 2023.

Reichstein, M., Camps-Valls, G., Stevens, B., Jung, M., Denzler, J., Carvalhais, N., and Prabhat: Deep learning and process understanding for data-driven Earth system science, Nature, 566, 195–204, https://doi.org/10.1038/s41586-019-0912-1, 2019.

Saltelli, A.: Making best use of model evaluations to compute sensitivity indices, Comput. Phys. Commun., 145, 280–297, https://doi.org/10.1016/S0010-4655(02)00280-1, 2002.

Saltelli, A., Tarantola, S., and Chan, K. P.-S.: A quantitative model-independent method for global sensitivity analysis of model output, Technometrics, 1999.

Shi, G., Sun, W., Shangguan, W., Wei, Z., Yuan, H., Li, L., Sun, X., Zhang, Y., Liang, H., Li, D., Huang, F., Li, Q., and Dai, Y.: A China dataset of soil properties for land surface modelling (version 2, CSDLv2), Earth Syst. Sci. Data, 17, 517–543, https://doi.org/10.5194/essd-17-517-2025, 2025.

https://doi.org/10.5194/egusphere-2025-6076
Preprint. Discussion started: 4 February 2026


Sitch, S., Smith, B., Prentice, I. C., Arneth, A., Bondeau, A., Cramer, W., Kaplan, J. O., Levis, S., Lucht, W., Sykes, M. T., Thonicke, K., and Venevsky, S.: Evaluation of ecosystem dynamics, plant geography and terrestrial carbon cycling in the LPJ dynamic global vegetation model, Glob. Change Biol., 9, 161–185, https://doi.org/10.1046/j.1365-2486.2003.00569.x, 2003.

Smith, B., Prentice, I. C., and Sykes, M. T.: Representation of vegetation dynamics in the modelling of terrestrial ecosystems: comparing two contrasting approaches within European climate space, Glob. Ecol. Biogeogr., 10, 621–637, 2001.

Smith, B., Samuelsson, P., Wramneby, A., and Rummukainen, M.: A model of the coupled dynamics of climate, vegetation and terrestrial ecosystem biogeochemistry for regional applications, Tellus B, 63, 87–106, https://doi.org/10.1111/j.1600-0870.2010.00477.x, 2011.

Smith, B., Wårlind, D., Arneth, A., Hickler, T., Leadley, P., Siltberg, J., and Zaehle, S.: Implications of incorporating N cycling and N limitations on primary production in an individual-based dynamic vegetation model, Biogeosciences, 11, 2027–2054, https://doi.org/10.5194/bg-11-2027-2014, 2014.

Sobol′, I. M.: Global sensitivity indices for nonlinear mathematical models and their monte carlo estimates, Math. Comput. Simul., 55, 271–280, https://doi.org/10.1016/S0378-4754(00)00270-6, 2001.

Song, X., Bryan, B. A., Paul, K. I., and Zhao, G.: Variance-based sensitivity analysis of a forest growth model, Ecol. Model., 247, 135–143, https://doi.org/10.1016/j.ecolmodel.2012.08.005, 2012.

Sprugel, D. G., Ryan, M. G., Brooks, J. R., Vogt, K. A., and Martin, T. A.: Respiration from the organ level to the stand, in: Resource Physiology of Conifers, Elsevier, 255–299, https://doi.org/10.1016/B978-0-08-092591-2.50013-3, 1995.

Sumner, D. M. and Jacobs, J. M.: Utility of penman–monteith, priestley–taylor, reference evapotranspiration, and pan evaporation methods to estimate pasture evapotranspiration, J. Hydrol., 308, 81–104, https://doi.org/10.1016/j.jhydrol.2004.10.023, 2005.

Tao, F., Zhou, Z., Huang, Y., Li, Q., Lu, X., Ma, S., Huang, X., Liang, Y., Hugelius, G., Jiang, L., Doughty, R., Ren, Z., and Luo, Y.: Deep Learning Optimizes Data-Driven Representation of Soil Organic Carbon in Earth System Model Over the Conterminous United States, Front. Big Data, 3, 17, https://doi.org/10.3389/fdata.2020.00017, 2020.

Teckentrup, L.: The future of terrestrial carbon in australia, UNSW Sydney, https://doi.org/10.26190/UNSWORKS/24738, 2023.

Thevasundaram, K., Gallagher, J. J., Cherng, F., and Chang, M. C. Y.: Engineering nonphotosynthetic carbon fixation for production of bioplastics by methanogenic archaea, Proc. Natl. Acad. Sci. U.S.A., 119, e2118638119, https://doi.org/10.1073/pnas.2118638119, 2022.

Thonicke, K., Venevsky, S., Sitch, S., and Cramer, W.: The role of fire disturbance for global vegetation dynamics: Coupling fire into a dynamic global vegetation model, Glob. Ecol. Biogeogr., 10, 661–677, https://doi.org/10.1046/j.1466-822X.2001.00175.x, 2001.

https://doi.org/10.5194/egusphere-2025-6076
Preprint. Discussion started: 4 February 2026


Vazquez-Cruz, M. A., Guzman-Cruz, R., Lopez-Cruz, I. L., Cornejo-Perez, O., Torres-Pacheco, I., and Guevara-Gonzalez, R. G.: Global sensitivity analysis by means of EFAST and sobol' methods and calibration of reduced state-variable TOMGRO model using genetic algorithms, Comput. Electron. Agric., 100, 1–12, https://doi.org/10.1016/j.compag.2013.10.006, 2014.

Verrelst, J., Rivera, J. P., Van Der Tol, C., Magnani, F., Mohammed, G., and Moreno, J.: Global sensitivity analysis of the SCOPE model: What drives simulated canopy-leaving sun-induced fluorescence?, Remote Sens. Environ., 166, 8–21, https://doi.org/10.1016/j.rse.2015.06.002, 2015.

Verrelst, J., Vicent, J., Rivera-Caicedo, J. P., Lumbierres, M., Morcillo-Pallarés, P., and Moreno, J.: Global Sensitivity Analysis of Leaf-Canopy-Atmosphere RTMs: Implications for Biophysical Variables Retrieval from Top-of-Atmosphere Radiance Data, Remote Sens., 11, 1923, https://doi.org/10.3390/rs11161923, 2019.

Wainwright, H. M., Finsterle, S., Jung, Y., Zhou, Q., and Birkholzer, J. T.: Making sense of global sensitivity analyses, Comput. Geosci., 65, 84–94, https://doi.org/10.1016/j.cageo.2013.06.006, 2014.

Wang, B., Smith, B., Waters, C., Feng, P., and Liu, D. L.: Modelling changes in vegetation productivity and carbon balance under future climate scenarios in southeastern Australia, Sci. Total Environ., 924, 171748, https://doi.org/10.1016/j.scitotenv.2024.171748, 2024.

Whitehead, D., Kelliher, F. M., Lane, P. M., and Pollock, D. S.: Seasonal partitioning of evaporation between trees and understorey in a widely spaced pinus radiata stand, J. Appl. Ecol., 31, 528, https://doi.org/10.2307/2404448, 1994.

Wu, S.: A systematic review of climate policies in China: Evolution, effectiveness, and challenges, Environ. Impact Assess. Rev., 99, 107030, https://doi.org/10.1016/j.eiar.2022.107030, 2023.

Yu, E., Ma, J., and Sun, J.: Developing a climate prediction system over southwest China using the 8-km weather research and forecasting (WRF) model: System design, model calibration, and performance evaluation, Weather Forecast., 37, 1703–1719, https://doi.org/10.1175/WAF-D-21-0188.1, 2022.

Yuxi, W., Li, P., Yuemin, Y., and Tiantian, C.: Global vegetation-temperature sensitivity and its driving forces in the 21st century, Earth's Future, 12, e2022EF003395, https://doi.org/10.1029/2022EF003395, 2024.

Zaehle, S., Sitch, S., Smith, B., and Hatterman, F.: Effects of parameter uncertainties on the modeling of terrestrial biosphere dynamics, Glob. Biogeochem. Cycles, 19, 2004GB002395, https://doi.org/10.1029/2004GB002395, 2005.

Zandi, P., Xia, X., Yang, J., Liu, J., Remusat, L., Rumpel, C., Bloem, E., Krasny, B. B., and Schnug, E.: Speciation and distribution of chromium (III) in rice root tip and mature zone: The significant impact of root exudation and iron plaque on chromium bioavailability, J. Hazard. Mater., 448, 130992, https://doi.org/10.1016/j.jhazmat.2023.130992, 2023.

Zhao, A., Li, Z., Zou, L., Wu, J., Stan, K., and Sanchez-Azofeif, A.: Evaluating dynamic global vegetation models in China: Challenges in capturing trends in leaf area and gross primary

https://doi.org/10.5194/egusphere-2025-6076
Preprint. Discussion started: 4 February 2026


productivity, but effective seasonal variation representation, Earth Syst. Dynam., https://doi.org/10.5194/esd-2024-44, 2025.